Article

Structure-Guided Optimization of HIV Integrase Strand Transfer Inhibitors

Xue Zhi Zhao, Steven J Smith, Daniel P Maskell, Mathieu Métifiot, Valerie E Pye, Katherine Fesen, Christophe Marchand, Yves Pommier, Peter Cherepanov, Stephen H Hughes, and Terrence R Burke

Just Accepted

Structure-Guided Optimization of HIV Integrase Strand Transfer Inhibitors

Xue Zhi Zhao,[1] Steven J. Smith,[2] Daniel P. Maskell,[4] Mathieu Métifiot,[3] Valerie E. Pye,[4]

Katherine Fesen,[3] Christophe Marchand,[3] Yves Pommier,[3] Peter Cherepanov,[4,5] Stephen H.

Hughes[3] and Terrence R. Burke, Jr.[1,*]

[1] Chemical Biology Laboratory and [2]HIV Dynamics and Replication Program, Center for

Cancer Research, National Cancer Institute, National Institutes of Health, Frederick, MD

21702 and [3]Developmental Therapeutics Branch and Laboratory of Molecular

Pharmacology, Center for Cancer Research, National Cancer Institute, National Institutes of

Health, Bethesda, MD 20892 and [4]Chromatin Structure and Mobile DNA, The Francis Crick

Institute, London, NW1 1AT, UK and [5]Imperial College London, St-Mary's Campus, Norfolk

Place, London, W2 1PG, UK.

_____

*Corresponding Author: Tel: 301-846-5906, Fax: 301-846-6033

E-mail: burkete@helix.nih.gov

1

ABSTRACT

Integrase mutations can reduce effectiveness of the first-generation FDA-approved integrase strand transfer inhibitors (INSTIs), raltegravir (RAL) and elvitegravir (EVG). The second-generation agent, dolutegravir (DTG) has enjoyed considerable clinical success; however, resistance-causing mutations that diminish the efficacy of DTG have appeared. Our current findings support and extend the substrate envelope concept that broadly effective INSTIs can be designed by filling the envelope defined by the DNA substrates. Previously, we explored 1-hydroxy-2-oxo-1,2-dihydro-1,8-naphthyridine-3-carboxamides as an INSTI scaffold, making a limited set of derivatives, and concluded that broadly effective INSTIs can be developed using this scaffold. Herein, we report an extended investigation of 6-substituents as well the first examples of 7-substituted analogs of this scaffold. While 7-substituents are not well-tolerated, we have identified novel substituents at the 6-position that are highly effective, with the best compound (**6p**) retaining better efficacy against a broad panel of known INSTI resistant mutants than any analogs we have previously described.

2

INTRODUCTION

HIV-1 integrase (IN) plays a key role in the viral life cycle, inserting the double-stranded DNA that is generated by reverse transcription of the viral RNA genome into the genome of the host cell.[1] Integration is essential for viral replication, and for this reason, IN is a therapeutic target for the treatment of HIV infections. To date, three HIV IN antagonists have been approved for clinical use: raltegravir (RAL, **1**), elvitegravir (EVG, **2**) and dolutegravir (DTG, **3**) (Figure 1).[2-4] These drugs belong to a class of compounds called integrase strand transfer inhibitors (INSTIs) because they inhibit DNA strand transfer (ST), the second step of integration catalyzed by IN, rather than the first step, 3'-processing reaction (3'-P).[5-8] Development of drug resistance mutations is a common problem in antiviral therapy and not surprisingly, mutations affecting the susceptibility of the virus to RAL and EVG have rapidly emerged.[9-11] However, the second-generation inhibitor, DTG retains potency against some but not all RAL/EVG resistant HIV variants.[12-16] Therefore, the development of new small molecules that have minimal toxicity and improved efficacy against the existing resistant mutants remains an important research objective.[17]

Retroviral integration is mediated by IN multimers that are assembled on the viral DNA ends forming a stable synaptic complex, also referred to as the intasome. [18-21] The INSTIs only bind to the active site of IN when the processed viral DNA ends are appropriately bound to the intasome.[8, 22] The way in which INSTIs bind to the intasome was elucidated by solving crystal structures of the orthologous retroviral IN from the prototype foamy virus (PFV).[19, 23, 24] The INSTIs are "interfacial" inhibitors; they bind to the active site of IN and interact with the bound viral DNA following the 3'-processing step.[8, 19, 25]

3

Essential structural features that contribute to the binding of INSTIs include an array of three heteroatoms (highlighted in red, Figure 1) that chelate the two catalytic Mg^{2+} ions in the IN active site and a halobenzyl side chain (halophenyl portion highlighted in blue, Figure 1) that stacks with the penultimate nucleotide (a deoxycytidine) at the 3' end of the viral DNA.[8, 19] We have recently shown that the 1-hydroxy-2-oxo-1,2-dihydro-1,8-naphthyridine-3-carboxamide motif (**4**) can serve a useful platform for developing HIV-1 IN inhibitors that retain high efficacy against the RAL/EVG-resistant mutants.[26, 27] We initially examined the properties of a series of analogs related to structure **4** by varying the substituents at the 4-position. Our objective was to identify compounds that retain efficacy against the mutations Y143R, N155H and Q148H/G140S, which have been associated with clinical resistance to RAL[27] and some of these mutations also play a role in the development of resistance against DTG.[28] This approach yielded compounds including **4a–d**, which are approximately equivalent to RAL in their potency against recombinant wild-type (WT) HIV-1 IN in biochemical assays. However, the small molecules also showed improved antiviral efficacies against the Y143R and N155H mutants in cell-based assays.[26, 27] Although antiviral efficacies against the Q148H/G140S double mutant were also improved relative to RAL, the new compounds were inferior to DTG, prompting us to continue our developmental efforts.

Structural studies using the PFV intasome have revealed that the tricyclic system of DTG is sufficiently extended to make contacts with G187 in the β4–α2 loop of PFV IN (G118 in IN).[23] It has been argued that the interactions with this region may contribute to the improved properties of DTG and other second-generation INSTIs.[4, 23, 29, 30] Therefore, we

4

considered that adding functionality to either the 6- or 7-positions of **4** could interact with the same region of the catalytic site (highlighted in green and cyan, respectively in the structures of DTG and **4**, Figure 1). In a preliminary work, we modified the 6-position of **4** and showed that adding linear side chains bearing terminal hydroxyl groups can improve antiviral efficacies against the Q148H/G140S double mutant to levels approaching that of DTG.[31] Furthermore, depending on the 6-substituent, compounds could retain essentially all of their antiviral potency against a more extensive panel of HIV-1 based vectors that carry the major DTG-resistant IN mutants, including the G118R, T66I, E92Q, R263K, H51Y single mutants and the H51Y/R263K double mutant.[17, 32-34] These data have two important implications: First, 6-substituents can have an important role in maintaining antiviral efficacy against resistant mutant forms of IN. Second, compounds that are broadly effective against mutant forms of IN bind in ways that involve substrate mimicry and when bound, fit within the "substrate envelope".[31, 35] However, the data were confined to a small number of 6-modificaitons that had limited chemical diversity. Given the potential promise of 6-substituents, we felt that it was important to more thoroughly examine this position and accordingly, we describe here an extensive set of 6-modifications (designated as the **6** series analogs, Figure 1). We were also interested in examining substituents at the 7-position of **4**, since these could potentially afford an alternate way to engage G118 in the β4–α2 loop of IN. We present the first examination of compounds that have modifications at the 7-position (designated as the **5** series analogs). To provide a more complete SAR study, we have also introduced various functionalities at the 4-position in combination with various 6- and 7-substitutents. These efforts have resulted in one of the most potent and effective compounds that we have developed to date. This work sheds additional light

5

on enzyme-inhibitor interactions that can contribute to retention of efficacy against strains

of virus that contain mutant forms of IN resistant to the approved INSTIs.

RESULTS AND DISCUSSION

Chemistry. To prepare our 7-substituted analogs **5a–i**, we employed 2,6-dichloronicotinic

acid (**7**) as starting material. The 6-chloro group of **7** was converted into the final 7-

substituent in two ways. In one route, the 6-chloro moiety was displaced with methoxyl

(KO^{t}Bu in MeOH)[36] and this was followed by esterification of the 3-carboxy group to yield **8**

(Scheme 1). In the second route, the 3-carboxyl group of **7** was first converted directly to

the 3-methyl ester. In both cases, the 2-chloro group was then displaced with BnONH$_2$ to

give the corresponding 2-benzyloxyamine-containing derivatives (**10a** and **9**, respectively).

The 6-chloro-substituents of the second series **9** were transformed into the corresponding

6-piperidinyl and 6-morpholino derivatives (**10b** and **10c**, respectively) by heating with

DMF solutions of piperidine or morpholine. Using a procedure similar to those we

previously reported (Scheme 1),[26, 27, 31] intermediates **10a–c** were transformed to the 4-

hydroxy (**5a–c**), 4-amino (**5d–f**) and 4-[2-(methyl glycinate)] (**5g–i**) final products.

(Insert Scheme 1)

We transformed the 6-bromo analogs (**17a–c,** Scheme 2) into a variety of 6-

substituted INSTIs by coupling alkynes and alkenes using Sonogashira and Heck coupling

chemistries.[31] In addition to the 6-substituted products with a 4-hydroxyl (**6a**), we

prepared analogs having a free amine at the 4-position (**6b–p**) as well as analogs with 4-[2-

(methyl glycinate)]amine (**6q**) and 4-(2-hydroxyethyl)amine (**6r–t**) (Scheme 2).

(Insert Scheme 2)

6

Evaluation of New Derivatives Using *In Vitro* IN Catalytic Assays and Single-Round

Virus Replication Assays. We designed compounds **5a–i** to examine the effects of

substituents at the 4-position (hydroxyl, amine, or methyl glycinate) in combination with

modifications of the 7-position (methoxyl, piperidinyl or morpholino). We evaluated the

compounds by *in vitro* IN activity assays that utilize ^{32}P-radiolabeled oligonucleotides

(Table 1).[37] We also tested the potency of the compounds in single-round replication assays

that employ HIV-1 vectors carrying WT IN. We evaluated the antiviral potencies of a subset

of the compounds against HIV-1 vectors carrying the canonical Y143R, N155H and

Q148H/G140S mutations that are associated with high-level HIV-1 resistance to RAL and

virological failure in patients (Table 2).[17, 32-34, 38, 39] As we recently reported, compounds

that lack substituents at the 6- and 7-positions and harboring a hydroxyl group at the 4-

position (**5'a**) showed lower potencies in the ST assay and poorer antiviral potencies than

the corresponding 4-amino-containing compound (**5'd**) (Tables 1 and 2).[26, 27] In our

current work, we found that a compound with a 4-[2-(methyl glycinate)] modification of

the 4-amino group (**5'g**) retained its enzymatic potency in these assays relative to **5'd**.

Bulky substituents at the 7-position (**5b**, **5c**, **5e**, **5f**, **5h** and **5i**, Table 1) diminished potency

by three-orders-of-magnitude relative to the corresponding unsubsituted analogs (**5'a**, **5'd**

and **5'g**, respectively). Although a 7-methoxyl group was better tolerated (compare with **5a**,

5d and **5g**), in all cases there was a reduction in the antiviral potency (Table 2).

(Insert Table 1)

(Insert Table 2)

7

We recently described a series of structurally related 4-amino-containing INSTIs, which possess 6-substituents consisting of primary hydroxyl or sulfone groups tethered by alkyl chains of various lengths.[31] The chemical diversity of these substituents was limited. To extend the diversity of the modifications at the 6-position, our current study examines analogs containing tethered acetoxy (**6b**), benzyloxy (**6c**), cyclohexyl (**6d**), phenyl (**6e** and **6f**), dimethylamino (**6g**), carboxyl (**6i**), methyl ester (**6p**) and carboxamido having a variety of alkylamide groups (**6j** – **6o**) groups (Tables 1and 2). Several of the resulting compounds retained low-nanomolar IC_{50} values in ST reactions. *N,N*-Dimethylpropylamine (**6g**, ST IC_{50} = 14 nM), propanoic acid (**6i**) propanoic amides (**6j** – **o**) and propanoic acid methyl ester (**6p**), as well as the reverse ester **6b** displayed IC_{50} values of 10 nM or less in the ST assay. Tethering a phenyl ring with an ethylene chain maintained good inhibitory potency (**6f**, ST IC_{50} = 14 nM). However, appending phenyl or cyclohexyl groups by increasing spacer lengths reduced potency by as much as three orders-of magnitude: three methylenes (cyclohexyl-containing **6d**, ST IC_{50} = 3.3 µM), four methylenes (phenyl-containing **6e**, ST IC_{50} = 2.0 µM) or longer (**6c**, ST IC_{50} = 3.3 µM) (Table 1). This result contrasts with our previous finding that appending a phenyl ring using a three-unit chain that contains a sulfone moiety can result in retention of high potency. In the latter case, a co-crystal structure with the PFV intasome revealed that the sulfone group causes the phenyl ring to adopt an unusual π–π stacking orientation, in which it is folded up under the naphthyridine ring system and fill the catalytic space more completely.[31]

Most 6-substituted analogs in our current study showed low nanomolar potencies against the WT enzyme in the *in vitro* ST assay and against a WT HIV-1 vector in the single-

8

round infectivity assay (Tables 1 and 2, respectively). However, for the 6-tethered 2-hydroxyethylamides (**6n** and **6o**), *in vitro* ST inhibitory potencies and antiviral potencies against a vector that replicates using WT IN differed considerably (IC$_{50}$ < 10 nM as compared to EC$_{50}$ ≥ 200 nM). Additionally, while analogs **6c, 6d** and **6e** showed micromolar ST-inhibitory potencies in the *in vitro* assay, they were significantly more potent in the antiviral assay. The reasons for these discrepancies are not clear. Among the remaining compounds, **6p**, with a 6-$(CH_2)_2CO_2CH_3$ substituent, exhibited the best antiviral profile against the panel of resistant mutants (Table 2). This derivative displayed a modest improvement in antiviral potency against a vector carrying a WT IN (EC$_{50}$ = 0.67 nM) as compared to **6'b**, which had been the most promising compound in work we recently reported.[31] Inhibitor **6'b** contains a 6-$(CH_2)_5OH$ group and a primary amine at the 4-position. Adding 4-[2-(methyl glycinate)] or 2-hydroxyethyl substituents to the 4-amino group of **6'b** did not improve the inhibitory profiles (compounds **6q** and **6r**, respectively), nor were the antiviral potencies improved by the addition of a 2-hydroxyethyl substituent to the 4-amino group of **6p** to yield **6t** (Tables 2). Most 6-subsituted analogs were not cytotoxic within the range tested (Table 2). Exceptions were found with **6c, 6d** and **6e**, which also showed anomalous discrepancies between their *in vitro* and antiviral potencies and with **6f** and **6g**. The reasons for the greater cytotoxicities of these analogs are not clear.

An important component of our current study is to test the effects of substituents at the 7-position. Given proximity to the metal-chelating 8-aryl nitrogen, we were uncertain of what the effects such modifications would have. Bulky groups at the 7-position (**5b, 5c, 5e, 5f, 5h** and **5i**) resulted in from two- to three-orders of magnitude loss of inhibitory potency

9

against the WT enzyme *in vitro*. These latter data were consistent with the bulky

substituents causing a disruption of essential interactions with the catalytic metal ions. Of

greater interest was our finding that 7-OCH$_3$ substituents were well tolerated against WT

enzyme in *in vitro* assays (see **5a**, **5d** and **5g**, Table 1).

Potencies of the New Compounds Against an Extended Set of Drug Resistant IN

Mutants. We selected a subset of the analogs (**6b**, **6p**, **6r**, **6s** and **6t**) for additional

evaluation in single-round viral replication assays using HIV-1 vectors harboring single

G118R, T66I, E92Q, R263K, H51Y, or the double H51Y/R263K substitutions associated

with DTG resistance (Table 3).[17, 32-34, 38, 39] For comparison, we also included **6'b**, which was

one of the most broadly effective of our previously reported inhibitors.[31] The new

compounds showed good antiviral potencies against the entire panel of mutants. Although

several compounds appear to be promising, the most potent analog (by a small margin)

was the 6-methyl 3-propanoate-containing **6p**, which showed a slightly better inhibitory

profile against the first panel of mutants (Table 2), while also retaining greater inhibitory

potency than DTG against the second, more extended panel of mutants (Table 4).

(Insert Table 3)

(Insert Table 4)

Crystal Structures of the PFV Intasome in Complex with 5'g, 5g and 6p. To understand

how some of the current analogs interact with the active site of IN, we soaked PFV

intasome crystals in the presence of **5'g**, **5g** or **6p** and refined the resulting structures

(Table 5). We recently described a crystal structure of **5'd** bound to the active site of PFV

10

intasome.[31] The inhibitor **5'g** bound to PFV IN differs from the previously reported **5'd**

structure only in having a *N*-(methyl 2-glycinate)amine moiety at its 4-position, and,

predictably, the two compounds bind to the active site in a very similar fashion.

Superposition with the DTG-bound structure confirmed that 8-naphthyridine nitrogen and

1-*N*-hydroxyl of **5'g** take the place of the 6-oxo and 7-hydroxyl heteroatoms of DTG. The

naphthyridine 2-oxo carbonyl of **5'g** corresponds to the ring 8-oxo carbonyl of DTG (Figure

2A).[23] However, the 4-*N*-(methyl 2-glycinate)amine group of **5'g** extends into the region

which is occupied by the first base of the scissile dinucleotide in viral DNA prior to 3'-P

(designated A18 in the crystal structure, Figure 2A), which may be related to the ability of

the compound to inhibit the 3'-P reaction.[8] Therefore, an extended form of substrate

mimicry may arise from the modification at the 4-position of **5'g**, which was not seen in the

co-crystal structure of **5'd**.[31] The idea that inhibitors that remain within the "substrate

envelope" are particularly effective against resistant forms of the target enzyme was

proposed by Schiffer and colleagues and is based on the idea that to be able to support viral

replication, any mutant form of a viral enzyme must be capable of binding its normal

substrate(s).[35] Thus, if the bound inhibitor remains within an envelope defined by the

substrate(s), the inhibitor is expected to retain some efficacy against mutant forms of the

enzyme.[40] Even though the original hypothesis was based on work with protease inhibitors,

it seems likely that this principle can be applied broadly to anti-viral compounds that bind

at the active sites of essential viral enzymes. The 4-*N*-(methyl 2-glycinate) amine group of

5'g is situated near (within 5 Å) to the side chains of Y212 and P214 (residues

corresponding to Y143 and P145 in HIV-1 IN) and to the adenosine base of the 3' terminal

viral DNA residue (A17), which adopts two alternative conformations in the crystal

11

structure (Figure 2B). The interactions with the side chains are much less extensive in the

cases of DTG (**3**) and **5'd**. Extension into this region of the catalytic site is also seen with

several highly potent INSTIs having diverse structures (see Figure S1 in Supporting

Information).

(Insert Figure 2)

Prior structural studies of the PFV intasome showed that the tricyclic system of DTG

makes contacts with G187 in the β4–α2 loop of PFV IN (G118 in IN) and it has been argued

that the interactions with this region may contribute to the improved properties of DTG

and other second-generation INSTIs. [4, 23, 29, 30] As has already been discussed, we thought

that it might be possible to make useful contacts with the same region of the catalytic site

by adding functionality to the 6- and 7-positions of **4**. To this end, we introduced

substituents at the 6- and 7-positions of **4** that could potentially recapitulate some of the

desirable features of DTG (highlighted in green and cyan, respectively in the structures of

DTG and **4**, Figure 1). We obtained the crystal structure of **6p** bound to the PFV intasome,

because it represents the most potent 6-substituted analog in our current study. The

structure revealed that the 6-methyl 3-propanoate side chain of the compound is situated

within the region defined by an envelope defined by both the pre-3'-P viral DNA and the

host target DNA substrate (Figure 3). This is consistent with our recent report that 6-

substituents of the compounds exhibiting the best antiviral profiles against the panel of

resistant mutants bind within an envelope defined as the confluence of viral DNA

substrates.[31] The structure also shows that the methyl carboxylate group of **6p** makes van

der Waals interactions with the β4–α2 loop of IN, becoming sandwiched between main

12

chain atoms of Q186 and G187 (residues corresponding to HIV-1 N117 and G118,

respectively) and the side chain of Y212 (Figure 4).

(Insert Figure 3)

(Insert Figure 4)

To understand the effects of introducing a 7-OCH$_3$ substituent, we solved the

structure of **5g** bound to the PFV intasome and overlaid the corresponding structure of

DTG bound to the PFV intasome (Figure 4). We observed that the 7-OCH$_3$ group of **5g** is

approximately 3.6 Å from the G187 residue in the β4–α2 loop, which compares favorably

with DTG and **6p** (approximately 3.9 Å and 3.7 Å, respectively, Figure 4A). The 7-OCH$_3$

group of **5g** did not appear to significantly alter the position of the metal chelating

heteroatoms of **5g** relative to **6p**. However, it is not immediately obvious why **5g** is more

susceptible to the N155H mutation compared to **6p** or to the more closely related **5'g**. Since

the N155 residue of HIV-1 IN corresponds to N224 in PFV IN, the X-ray crystal structure

with the mutation N224H in PFV IN did show that the side chain of His224 interacts with a

phosphoryl oxygen atom in viral DNA and that INSTI binding is accompanied by a loss of

this contact.[24] The associated energetic penalty may explain the loss potency of some

compounds against N155H HIV-1 IN. In the co-crystal structure of PFV intasome with **5g,**

the location of this phosphoryl oxygen is nearly identical to that seen for **6p**, **5'g** and DTG

(Figure 4C). The abilities of some INSTIs to re-adjust in the active site of IN may help

explain variations among in their susceptibilities of the different INSTIs to the N155H

mutation.[23, 24, 41]

13

CONCLUSIONS

Earlier, we reported that the 1-hydroxy-2-oxo-1,2-dihydro-1,8-naphthyridine-3-carboxamide scaffold represents a potentially attractive platform for the development of INSTIs, that retain good antiviral efficacy against a panel of viral vectors carrying resistant mutant forms of IN.[26, 27] More recently, we began an exploration of the effects of modifying the 6-position of our earlier compounds.[31] We found that 6-substituents may play an important role in enhancing the maintenance of antiviral efficacy against drug-resistant mutant forms of IN. Furthermore, the most broadly effective compounds are substrate mimics that fit within the "substrate envelope." Our original purpose in synthesizing 6-substituents was to create additional interactions within areas of the catalytic region accessed by the third ring of DTG. However, the range of functionality reported in the prior paper was quite limited, consisting of primary hydroxyl groups tethered by linear polymethylene chains of varying lengths, and a single tethered phenyl sulfone. We now report a much more extensive exploration of functionalities at the 6-position, as well as the first examination of derivatives with modifications at the 7-position. We also tested whether the compounds could be improved by introduced by varying functionalities at the 4-position.

We observed that -OCH_3 groups are somewhat better tolerated than bulky subsituents at the 7-position when examined *in vitro* against WT enzyme. However, compounds with 7-OMe groups showed significantly reduced antiviral potency when tested against viral vectors that carry the N155H mutation. We found that a variety of substituents can be added at the 6-position, which enhance the antiviral potencies of the

14

compounds against the major RAL, EVG and DTG-resistant IN mutants. Many of these

compounds are not cytotoxic at the tested concentrations, and the best analog, **6p**, is the

most effective in terms of its ability to inhibit the entire spectrum of IN mutants of any of

the compounds we have described. The crystal structure of the PFV intasome with **6p**

bound supports the idea that interactions with the $\beta4$–$\alpha2$ loop are important and that

compounds that bind within the envelope defined by both the viral and host DNA

substrates helps the compounds retain broad efficacy. We found that the 4-amine

substituent in **5'g** accesses a region of the active site of IN that would normally be occupied

by the base of the T_{+2} adenosine of the viral DNA prior to the 3'-P cleavage, providing

further support that binding within an envelope defined by the DNA substrates helps the

compounds retain broad efficacy. Thus, our results will inform the design and development

of next-generation INSTIs with broader efficacy against the known drug resistant mutants.

EXPERIMENTAL SECTION

General Procedures. Proton (^{1}H) and carbon (^{13}C) NMR spectra were recorded on

a Varian 400 MHz spectrometer or a Varian 500 MHz spectrometer and are reported in

ppm relative to TMS and referenced to the solvent in which the spectra were collected.

Solvent was removed by rotary evaporation under reduced pressure and anhydrous

solvents were obtained commercially and used without further drying. Purification by

silica gel chromatography was performed using Combiflash with EtOAc–hexanes solvent

systems. Preparative high pressure liquid chromatography (HPLC) was conducted using a

Waters Prep LC4000 system having photodiode array detection and Phenomenex C_{18}

columns (Cat. No. 00G-4436-P0-AX, 250 mm × 21.2 mm 10 μm particle size, 110 Å pore) at

15

a flow rate of 10 mL/min. Binary solvent systems consisting of A = 0.1% aqueous TFA and

B = 0.1% TFA in acetonitrile were employed with gradients as indicated. Products were

obtained as amorphous solids following lyophilization. Electrospray ionization-mass

spectrometric (ESI-MS) were acquired with an Agilent LC/MSD system equipped with a

multimode ion source. Purities of samples subjected to biological testing were assessed

using this system and shown to be ≥ 95%. High resolution mass spectrometric (HRMS)

were acquired by LC/MS-ESI using LTQ-Orbitrap-XL at 30K resolution.

General Procedure I for the Synthesis of Carboxamides (5a–i and 6a–t). Benzyl

protected compounds (**13**, **15**, **16** and **19**) (0.1 mmol) were suspended in methanol (10 mL)

and ethyl acetate (3 mL). Equivalent of Pd/C (10%) was added. The mixture was stirred at

room temperature under hydrogen. When the starting material was disappeared (TLC), the

crude mixture was filtered and washed by methanol. The filtrate was concentrated and

purified by HPLC to provide final carboxamides (**5a–i** and **6a–t**).

N-(2,4-Difluorobenzyl)-1,4-dihydroxy-7-methoxy-2-oxo-1,2-dihydro-1,8-

naphthyridine-3-carboxamide (5a). Treatment of **13a** as outlined in general procedure I,

and purification by preparative HPLC (with a linear gradient of 30% B to 90% B over 30

min; retention time = 25.5 min) provided **5a** as a white fluffy solid (22% yield). ^{1}H NMR

(400 MHz, DMSO-d_6) δ 11.00 (s, 1H), 10.42 (d, J = 5.8 Hz, 1H), 8.29 (dd, J = 8.7, 0.9 Hz, 1H),

7.48 (dd, J = 15.3, 8.6 Hz, 1H), 7.30 – 7.25 (m, 1H), 7.10 (dd, J = 9.8, 7.3 Hz, 1H), 6.83 – 6.81

(m, 1H), 4.62 (d, J = 6.0 Hz, 2H), 4.02 (s, 3H). ESI-MS m/z: 378.1 (MH$^+$).

N-(2,4-Difluorobenzyl)-1,4-dihydroxy-2-oxo-7-(piperidin-1-yl)-1,2-dihydro-

1,8-naphthyridine-3-carboxamide (5b). Treatment of **13b** as outlined in general

16

procedure I, and purification by preparative HPLC (with a linear gradient of 50% B to 90% B over 30 min; retention time = 24.0 min) provided **5b** as a white fluffy solid (13% yield). ^{1}H NMR (400 MHz, DMSO-d_6) δ 10.52 (bs, 1H), 10.36 (t, *J* = 5.9 Hz, 1H), 7.93 (d, *J* = 9.1 Hz, 1H), 7.41 (dd, *J* = 15.3, 8.7 Hz, 1H), 7.25 – 7.19 (m, 1H), 7.04 (dd, *J* = 9.3, 6.7 Hz, 1H), 6.82 (d, *J* = 9.2 Hz, 1H), 4.54 (d, *J* = 5.8 Hz, 2H), 3.74 (s, 4H), 1.61 (bs, 2H), 1.52 (bs, 4H). ESI-MS *m/z*: 431.2 (MH+).

N-(2,4-Difluorobenzyl)-1,4-dihydroxy-7-morpholino-2-oxo-1,2-dihydro-1,8-naphthyridine-3-carboxamide (5c). Treatment of **13c** as outlined in general procedure I, and purification by preparative HPLC (with a linear gradient of 30% B to 90% B over 30 min; retention time = 24.3 min) provided **5c** as a white fluffy solid (30% yield). ^{1}H NMR (400 MHz, DMSO-d_6) δ 10.60 (s, 1H), 10.36 (t, *J* = 6.0 Hz, 1H), 8.01 (d, *J* = 9.1 Hz, 1H), 7.41 (dd, *J* = 15.3, 8.6 Hz, 1H), 7.25 – 7.19 (m, 1H), 7.06 – 7.02 (m, 1H), 6.83 (d, *J* = 9.1 Hz, 1H), 4.54 (d, *J* = 6.0 Hz, 2H), 3.73 (s, 4H), 3.65 (t, *J* = 4.5 Hz, 4H). ESI-MS *m/z*: 433.1 (MH+).

4-Amino-N-(2,4-difluorobenzyl)-1-hydroxy-7-methoxy-2-oxo-1,2-dihydro-1,8-naphthyridine-3-carboxamide (5d). Treatment of **16a** as outlined in general procedure I, and purification by preparative HPLC (with a linear gradient of 30% B to 75% B over 30 min; retention time = 22.4 min) provided **5d** as a white fluffy solid (37% yield). ^{1}H NMR (400 MHz, DMSO-d_6) δ 10.60 (t, *J* = 5.6 Hz, 1H), 10.51 (bs, 1H), 8.48 (d, *J* = 8.8 Hz, 1H), 7.38 (dd, *J* = 15.4, 8.7 Hz, 1H), 7.22 – 7.17 (m, 1H), 7.02 (td, *J* = 8.5, 2.5 Hz, 1H), 6.72 (d, *J* = 8.8 Hz, 1H), 4.46 (d, *J* = 5.7 Hz, 2H), 3.94 (s, 3H). ESI-MS *m/z*: 377.1 (MH+).

4-Amino-N-(2,4-difluorobenzyl)-1-hydroxy-2-oxo-7-(piperidin-1-yl)-1,2-dihydro-1,8-naphthyridine-3-carboxamide (5e). Treatment of **16b** as outlined in

general procedure I, and purification by preparative HPLC (with a linear gradient of 50% B

to 70% B over 30 min; retention time = 20.6 min) provided **5e** as a white fluffy solid (49%

yield). ^{1}H NMR (400 MHz, DMSO-d_6) δ 10.63 (t, J = 5.8 Hz, 2H), 8.19 (d, J = 9.2 Hz, 1H), 7.36

(dd, J = 15.4, 8.7 Hz, 1H), 7.21 – 7.16 (m, 1H), 7.02 (t, J = 9.0 Hz, 1H), 6.75 (d, J = 9.2 Hz, 1H),

4.44 (d, J = 5.7 Hz, 2H), 3.69 (bs, 4H), 1.59 (bs, 2H), 1.50 (bs, 4H). ESI-MS m/z: 430.2 (MH$^+$).

4-Amino-N-(2,4-difluorobenzyl)-1-hydroxy-7-morpholino-2-oxo-1,2-dihydro-

1,8-naphthyridine-3-carboxamide (5f). Treatment of **16c** as outlined in general

procedure I, and purification by preparative HPLC (with a linear gradient of 30% B to 65%

B over 30 min; retention time = 24.0 min) provided **5f** as a white fluffy solid (28% yield). ^{1}H

NMR (400 MHz, DMSO-d_6) δ 10.62 (t, J = 5.7 Hz, 1H), 10.27 (bs, 1H), 10.19 (bs, 1H), 8.26 (d,

J = 9.1 Hz, 1H), 7.36 (dd, J = 15.4, 8.7 Hz, 1H), 7.21 – 7.16 (m, 1H), 7.02 (td, J = 8.2, 2.0 Hz,

1H), 6.76 (d, J = 9.1 Hz, 1H), 4.44 (d, J = 5.7 Hz, 2H), 3.66 (d, J = 3.3 Hz, 8H). ESI-MS m/z:

432.1 (MH$^+$).

Methyl 2-((3-((2,4-Difluorobenzyl)carbamoyl)-1-hydroxy-7-methoxy-2-oxo-

1,2-dihydro-1,8-naphthyridin-4-yl)amino)acetate (5g). Treatment of **15a** as outlined in

general procedure I, and purification by preparative HPLC (with a linear gradient of 30% B

to 80% B over 30 min; retention time = 23.7 min) provided **5g** as a white fluffy solid (20%

yield). ^{1}H NMR (400 MHz, DMSO-d_6) δ 11.17 (bs, 1H), 10.61 (bs, 1H), 10.45 (t, J = 5.7 Hz,

1H), 8.31 (d, J = 9.0 Hz, 1H), 7.45 (dd, J = 15.3, 8.7 Hz, 1H), 7.22 – 7.17 (m, 1H), 7.02 (td, J =

8.5, 1.6 Hz, 1H), 6.65 (d, J = 8.9 Hz, 1H), 4.48 (d, J = 5.4 Hz, 2H), 4.45 (d, J = 5.9 Hz, 2H), 3.94

(s, 3H), 3.63 (s, 3H). ESI-MS m/z: 449.1 (MH$^+$).

Methyl 2-((3-((2,4-Difluorobenzyl)carbamoyl)-1-hydroxy-2-oxo-7-(piperidin-

1-yl)-1,2-dihydro-1,8-naphthyridin-4-yl)amino)acetate (5h). Treatment of **15b** as

18

outlined in general procedure I, and purification by preparative HPLC (with a linear

gradient of 50% B to 70% B over 30 min; retention time = 22.9 min) provided **5h** as a white

fluffy solid (29% yield). ^{1}H NMR (400 MHz, DMSO-d_6) δ 11.45 (bs, 1H), 10.70 (t, J = 5.7 Hz,

1H), 7.98 (d, J = 9.4 Hz, 1H), 7.39 (dd, J = 15.3, 8.7 Hz, 1H), 7.22 – 7.16 (m, 1H), 7.02 (td, J =

8.6, 2.1 Hz, 1H), 6.65 (d, J = 9.4 Hz, 1H), 4.45 (bs, 2H), 4.44 (s, 2H), 3.70 (bs, 4H), 3.64 (s, 3H),

1.60 (bs, 3H), 1.51 (bs, 3H). ESI-MS m/z: 502.2 (MH$^+$).

Methyl 2-((3-((2,4-Difluorobenzyl)carbamoyl)-1-hydroxy-7-morpholino-2-

oxo-1,2-dihydro-1,8-naphthyridin-4-yl)amino)acetate (5i). Treatment of **15c** as

outlined in general procedure I, and purification by preparative HPLC (with a linear

gradient of 30% B to 70% B over 30 min; retention time = 26.0 min) provided **5i** as a white

fluffy solid (18% yield). ^{1}H NMR (400 MHz, DMSO-d_6) δ 11.43 (bs, 1H), 10.66 (t, J = 5.8 Hz,

1H), 10.31 (bs, 1H), 8.06 (d, J = 9.3 Hz, 1H), 7.40 (dd, J = 15.4, 8.7 Hz, 1H), 7.21 – 7.16 (m,

1H), 7.02 (dd, J = 9.8, 7.4 Hz, 1H), 6.66 (d, J = 9.3 Hz, 1H), 4.47 (d, J = 5.4 Hz, 2H), 4.45 (d, J =

5.7 Hz, 2H), 3.66 (d, J = 5.2 Hz, 8H), 3.63 (s, 3H). ESI-MS m/z: 504.2 (MH$^+$).

N-(2,4-Difluorobenzyl)-1,4-dihydroxy-6-(5-hydroxypentyl)-2-oxo-1,2-

dihydro-1,8-naphthyridine-3-carboxamide (6a). Treatment of 1-(benzyloxy)-6-bromo-

N-(2,4-difluorobenzyl)-4-hydroxy-2-oxo-1,2-dihydro-1,8-naphthyridine-3-carboxamide

17a[31] with commercially available pent-4-yn-1-ol as outlined in general procedures J and I

and purification by preparative HPLC (linear gradient of 30% B to 70% B over 30 min;

retention time = 23.8 min) provided **6a** as a white fluffy solid (46% yield, two steps). ^{1}H

NMR (500 MHz, DMSO-d_6) δ 10.96 (bs, 1H), 10.52 (t, J = 6.1 Hz, 1H), 8.70 (d, J = 2.0 Hz, 1H),

8.26 (d, J = 2.0 Hz, 1H), 7.48 (dd, J = 15.3, 8.6 Hz, 1H), 7.30 – 7.25 (m, 1H), 7.09 (td, J = 8.5,

19

2.5 Hz, 1H), 4.63 (d, J = 5.9 Hz, 2H), 3.37 (t, J = 6.5 Hz, 2H), 2.73 (t, J = 7.6 Hz, 2H), 1.65 –

1.59 (m, 2H), 1.46 – 1.42 (m, 2H), 1.35 – 1.28 (m, 2H). ESI-MS m/z: 434.1 (MH$^+$). HRMS

calcd $C_{21}H_{22}F_2N_3O_5$ [MH$^+$], 434.1522; found, 434.1507.

3-(5-Amino-6-((2,4-difluorobenzyl)carbamoyl)-8-hydroxy-7-oxo-7,8-dihydro-

1,8-naphthyridin-3-yl)propyl Acetate (6b). Treatment of **19a** as outlined in general

procedure I and purification by preparative HPLC (linear gradient of 30% B to 70% B over

30 min; retention time = 20.6 min) provided **6b** as a white fluffy solid (71% yield). ^{1}H NMR

(500 MHz, DMSO-d_6) δ 10.69 (t, J = 5.7 Hz, 1H), 8.60 (s, 1H), 8.57 (s, 1H), 7.42 (dd, J = 15.6,

7.5 Hz, 1H), 7.24 (t, J = 9.9 Hz, 1H), 7.07 (t, J = 8.5 Hz, 1H), 4.52 (d, J = 5.5 Hz, 2H), 4.05 (t, J =

6.3 Hz, 2H), 2.75 (t, J = 7.9 Hz, 2H), 2.00 (s, 3H), 1.97 (d, J = 7.7 Hz, 2H). ESI-MS m/z: 447.1

(MH$^+$). HRMS calcd $C_{21}H_{21}F_2N_4O_5$ [MH$^+$], 447.1475; found, 447.1477.

6-(5-Amino-6-((2,4-difluorobenzyl)carbamoyl)-8-hydroxy-7-oxo-7,8-dihydro-

1,8-naphthyridin-3-yl)hexyl Benzoate (6c). Protection of 1-(benzyloxy)-N-(2,4-

difluorobenzyl)-4-((2,4-dimethoxybenzyl)amino)-6-(6-hydroxyhex-1-yn-1-yl)-2-oxo-1,2-

dihydro-1,8-naphthyridine-3-carboxamide[31] (50 mg, 0.073 mmol) using benzoic

anhydride (25 mg, 0.11 mmol) in pyridine (0.5 mL) (room temperature, 2 h) provided 6-(8-

(benzyloxy)-6-((2,4-difluorobenzyl)carbamoyl)-5-((2,4-dimethoxybenzyl)amino)-7-oxo-

7,8-dihydro-1,8-naphthyridin-3-yl)hex-5-yn-1-yl benzoate as a white solid (56 mg, 96%

yield). [^{1}H NMR (500 MHz, CDCl$_3$) δ 11.99 (t, J = 5.8 Hz, 1H), 10.69 (t, J = 5.8 Hz, 1H), 8.67 (d,

J = 1.4 Hz, 1H), 8.34 (d, J = 1.7 Hz, 1H), 8.07 – 8.05 (m, 2H), 7.39 – 7.68 (m, 2H), 7.57 (t, J =

7.4 Hz, 1H), 7.45 (t, J = 7.8 Hz, 2H), 7.40 – 7.36 (m, 4H), 7.23 (d, J = 8.9 Hz, 1H), 6.86 – 6.79

(m, 2H), 6.48 – 6.46 (m, 2H), 5.26 (s, 2H), 4.75 (d, J = 5.9 Hz, 2H), 4.60 (d, J = 5.6 Hz, 2H),

20

4.41 (t, *J* = 6.4 Hz, 2H), 3.81 (s, 3H), 3.78 (s, 3H), 2.54 (t, *J* = 7.0 Hz, 2H), 1.99 – 1.93 (m, 2H),

1.84 – 1.78 (m, 2H). ESI-MS *m/z*: 787.3 (MH+).] After treatment as outlined in general

procedure H and I and purification by preparative HPLC (linear gradient of 55% B to 75%

B over 30 min; retention time = 25.4 min), **6c** was provided as a white fluffy solid (45%

yield, two steps). ¹H NMR (500 MHz, DMSO-d_6) δ 10.69 (t, *J* = 5.7 Hz, 1H), 8.58 (d, *J* = 1.9 Hz,

1H), 8.54 (s, 1H), 7.94 (dd, *J* = 8.4, 1.3 Hz, 2H), 7.64 (dt, *J* = 8.7, 1.3 Hz, 1H), 7.53 – 7.50 (m,

2H), 7.42 (dd, *J* = 15.3, 8.5 Hz, 1H), 7.26 – 7.21 (m, 1H), 7.06 (dd, *J* = 9.8, 7.3 Hz, 1H), 4.51 (d,

J = 5.6 Hz, 2H), 4.26 (t, *J* = 6.5 Hz, 2H), 2.70 – 2.67 (m, 2H), 1.73 – 1.66 (m, 4H), 1.45 – 1.42

(m, 2H), 1.39-1.38 (m, 2H). ESI-MS *m/z*: 551.2 (MH+). HRMS calcd $C_{29}H_{29}F_2N_4O_5$ [MH+],

551.2089; found, 551.2089.

4-Amino-6-(3-cyclohexylpropyl)-*N*-(2,4-difluorobenzyl)-1-hydroxy-2-oxo-1,2-

dihydro-1,8-naphthyridine-3-carboxamide (6d). Treatment of **19b** as outlined in

general procedure I and purification by preparative HPLC (linear gradient of 50% B to 80%

B over 30 min; retention time = 27.5 min) provided **6d** as a white fluffy solid (40% yield).

¹H NMR (500 MHz, DMSO-d_6) δ 10.63 (t, *J* = 5.8 Hz, 1H), 8.51 (s, 1H), 8.47 (s, 1H), 7.36 (dd, *J*

= 15.5, 8.6 Hz, 1H), 7.20 – 7.15 (m, 1H), 7.00 (t, *J* = 8.5 Hz, 1H), 4.45 (d, *J* = 5.7 Hz, 2H), 2.59

(t, *J* = 7.7 Hz, 2H), 1.63 – 1.52 (m, 7H), 1.16 – 1.00 (m, 6H), 0.82 – 0.75 (m, 2H). ESI-MS *m/z*:

471.2 (MH+). HRMS calcd $C_{25}H_{29}F_2N_4O_3$ [MH+], 471.2202; found, 471.2204.

4-Amino-*N*-(2,4-difluorobenzyl)-1-hydroxy-2-oxo-6-(4-phenylbutyl)-1,2-

dihydro-1,8-naphthyridine-3-carboxamide (6e). Treatment of **19c** as outlined in

general procedure I and purification by preparative HPLC (linear gradient of 40% B to 80%

B over 30 min; retention time = 26.0 min) provided **6e** as a white fluffy solid (27% yield).

21

^{1}H NMR (500 MHz, DMSO-d_6) δ 10.69 (t, J = 5.8 Hz, 1H), 8.58 (s, 1H), 8.54 (s, 1H), 7.42 (dd, J = 15.5, 8.5 Hz, 1H), 7.26 (t, J = 7.6 Hz, 2H), 7.24-7.21 (m, 1H), 7.19-7.14 (m, 3H), 7.07 (t, J = 8.5 Hz, 1H), 4.51 (d, J = 5.7 Hz, 2H), 2.72 (t, J = 7.3 Hz, 2H), 2.62 (t, J = 7.5 Hz, 2H), 1.69 (dd, J = 14.8, 7.1 Hz, 2H), 1.65 – 1.53 (m, 2H). ESI-MS m/z: 479.2 (MH$^+$). HRMS calcd $C_{26}H_{25}F_2N_4O_3$ [MH$^+$], 479.1889; found, 479.1880.

4-Amino-*N*-(2,4-difluorobenzyl)-1-hydroxy-2-oxo-6-phenethyl-1,2-dihydro-1,8-naphthyridine-3-carboxamide (6f). Treatment of **19d** as outlined in general procedure I and purification by preparative HPLC (linear gradient of 40% B to 80% B over 30 min; retention time = 22.5 min) provided **6f** as a white fluffy solid (65% yield). ^{1}H NMR (500 MHz, DMSO-d_6) δ 10.69 (bs, 1H), 10.51 (bs, 1H), 8.61 (s, 1H), 8.53 (s, 1H), 7.45-7.42 (m, 1H), 7.35-7.32 (m, 1H), 7.27 (d, J = 7.0 Hz, 1H), 7.23 (d, J = 6.7 Hz, 2H), 7.20-7.17 (m, 1H), 7.08-7.05 (m, 1H), 4.52 (d, J = 5.5 Hz, 2H), 2.99 (bs, 4H). ESI-MS m/z: 451.1 (MH$^+$). HRMS calcd $C_{24}H_{21}F_2N_4O_3$ [MH$^+$], 451.1576; found, 451.1576.

4-Amino-*N*-(2,4-difluorobenzyl)-6-(3-(dimethylamino)propyl)-1-hydroxy-2-oxo-1,2-dihydro-1,8-naphthyridine-3-carboxamide (6g). Treatment of **19e** as outlined in general procedure I and purification by preparative HPLC (linear gradient of 30% B to 55% B over 30 min; retention time = 17.2 min) provided **6g** as a white fluffy solid (52% yield). ^{1}H NMR (500 MHz, DMSO-d_6) δ 10.68 (t, J = 5.8 Hz, 1H), 10.57 (s, 1H), 8.62 (s, 1H), 8.57 (s, 1H), 7.42 (dd, J = 15.5, 8.5 Hz, 1H), 7.27 – 7.22 (m, 1H), 7.07 (dd, J = 9.8, 7.3 Hz, 1H), 4.52 (d, J = 5.8 Hz, 2H), 3.06 (d, J = 7.7 Hz, 2H), 2.78 (s, 6H), 2.74 (t, J = 7.5 Hz, 2H), 2.01 (dt, J = 15.7, 7.8 Hz, 2H). ESI-MS m/z: 432.2 (MH$^+$). HRMS calcd $C_{21}H_{24}F_2N_5O_3$ [MH$^+$], 432.1842; found, 432.1824.

22

4-Amino-*N*-(2,4-difluorobenzyl)-1-hydroxy-6-(3-(2-hydroxyethoxy)propyl)-2-oxo-1,2-dihydro-1,8-naphthyridine-3-carboxamide (6h). Treatment of **19f** as outlined in general procedure I and purification by preparative HPLC (linear gradient of 30% B to 60% B over 30 min; retention time = 20.5 min) provided **6h** as a white fluffy solid (86% yield). ^{1}H NMR (500 MHz, DMSO-d_6) δ 10.69 (t, *J* = 5.8 Hz, 1H), 8.59 (d, *J* = 1.9 Hz, 1H), 8.56 (d, *J* = 1.9 Hz, 1H), 7.52 – 7.35 (m, 1H), 7.24 (ddd, *J* = 10.5, 9.4, 2.6 Hz, 1H), 7.07 (ddd, *J* = 10.4, 8.1, 2.2 Hz, 1H), 4.52 (d, *J* = 5.7 Hz, 2H), 3.51 (t, *J* = 5.3 Hz, 2H), 3.41 (dt, *J* = 7.5, 5.7 Hz, 4H), 2.76 – 2.73 (m, 2H), 1.92 – 1.86 (m, 2H). ESI-MS *m/z*: 449.1 (MH$^+$). HRMS calcd $C_{21}H_{23}F_2N_4O_5$ [MH$^+$], 449.1631; found, 449.1631.

3-(5-Amino-6-((2,4-difluorobenzyl)carbamoyl)-8-hydroxy-7-oxo-7,8-dihydro-1,8-naphthyridin-3-yl)propanoic Acid (6i). Treatment of **19g** with aqueous NaOH and then as outlined in general procedure I and purification by preparative HPLC (with a linear gradient of 30% B to 50% B over 30 min; retention time = 19.5 min) provided **6i** as a white fluffy solid (80% yield). ^{1}H NMR (400 MHz, DMSO-d_6) δ 10.63 (t, *J* = 5.4 Hz, 1H), 8.68 – 8.66 (m, 1H), 8.63 – 8.60 (m, 1H), 8.57 (d, *J* = 1.9 Hz, 1H), 8.53 (d, *J* = 1.9 Hz, 1H), 7.40 – 7.34 (m, 1H), 7.21 – 7.16 (m, 1H), 7.04 – 6.99 (m, 1H), 4.47 (d, *J* = 5.5 Hz, 2H), 2.87 (t, *J* = 7.5 Hz, 2H), 2.62 (t, *J* = 7.6 Hz, 2H). ESI-MS *m/z*: 419.1 (MH$^+$). HRMS calcd $C_{19}H_{17}F_2N_4O_5$ [MH$^+$], 419.1162; found, 419.1147.

4-Amino-*N*-(2,4-difluorobenzyl)-6-(3-(dimethylamino)-3-oxopropyl)-1-hydroxy-2-oxo-1,2-dihydro-1,8-naphthyridine-3-carboxamide (6j) and **(*E*)-4-Amino-*N*-(2,4-difluorobenzyl)-6-(3-(dimethylamino)-3-oxoprop-1-en-1-yl)-1-hydroxy-2-oxo-1,2-dihydro-1,8-naphthyridine-3-carboxamide (6k).** Treatment of **18e** as outlined

23

in general procedure I and H and purification by preparative HPLC (with a linear gradient

of 30% B to 45% B over 30 min) provided **6j** and **6k** as white fluffy solids. For **6j:** retention

time = 20.7 min. ^{1}H NMR (400 MHz, DMSO-d_6) δ 10.62 (t, J = 5.8 Hz, 1H), 10.46 (brs, 1H),

8.56 (d, J = 1.8 Hz, 1H), 8.50 (d, J = 1.8 Hz, 1H), 7.36 (dd, J = 15.4, 8.6 Hz, 1H), 7.20 – 7.14 (m,

1H), 7.00 (td, J = 8.6, 1.9 Hz, 1H), 4.45 (d, J = 5.7 Hz, 2H), 2.90 (s, 3H), 2.84 (t, J = 7.4 Hz, 2H),

2.74 (s, 3H), 2.65 (t, J = 7.5 Hz, 2H). ESI-MS m/z: 446.2 (MH$^+$). HRMS calcd $C_{21}H_{22}F_2N_5O_4$

[MH$^+$], 446.1634; found, 446.1617**.** For **6k**: retention time = 24.1 min. ^{1}H NMR (400 MHz,

DMSO-d_6) δ 10.63 (s, 1H), 10.53 (t, J = 5.8 Hz, 1H), 8.94 (s, 2H), 7.49 (d, J = 15.4 Hz, 1H),

7.37 (dd, J = 12.2, 5.3 Hz, 1H), 7.31 (d, J = 15.5 Hz, 1H), 7.21 – 7.15 (m, 1H), 7.01 (td, J = 8.9,

2.3 Hz, 1H), 4.46 (d, J = 5.7 Hz, 2H), 3.14 (s, 3H), 2.89 (s, 3H). ESI-MS m/z: 444.1 (MH$^+$).

HRMS calcd $C_{21}H_{20}F_2N_5O_4$ [MH$^+$], 444.1478; found, 444.1475**.**

4-Amino-*N*-(2,4-difluorobenzyl)-1-hydroxy-6-(3-(isopropylamino)-3-

oxopropyl)-2-oxo-1,2-dihydro-1,8-naphthyridine-3-carboxamide (6l) and **(*E*)-4-**

Amino-*N*-(2,4-difluorobenzyl)-1-hydroxy-6-(3-(isopropylamino)-3-oxoprop-1-en-1-

yl)-2-oxo-1,2-dihydro-1,8-naphthyridine-3-carboxamide (6m). Treatment of **18f** as

outlined in general procedure I and H and purification by preparative HPLC (with a linear

gradient of 30% B to 45% B over 30 min) provided **6l** and **6m** as white fluffy solids. For **6l**:

retention time = 23.0 min. ^{1}H NMR (400 MHz, DMSO-d_6) δ 10.62 (t, J = 5.7 Hz, 1H), 10.46

(brs, 1H), 8.50 (d, J = 1.8 Hz, 1H), 8.47 (s, 1H), 7.61 (d, J = 7.5 Hz, 1H), 7.36 (dd, J = 15.4, 8.7

Hz, 1H), 7.20-7.14 (m, 1H), 7.02-6.98 (m, 1H), 4.45 (d, J = 5.7 Hz, 2H), 3.76-3.68 (m, 1H),

2.84 (t, J = 7.5 Hz, 2H), 2.36 (t, J = 7.6 Hz, 2H), 0.90 (d, J = 6.6 Hz, 6H). ESI-MS m/z: 460.2

(MH$^+$). HRMS calcd $C_{22}H_{24}F_2N_5O_4$ [MH$^+$], 460.1791; found, 460.1772**.** For **6m**: retention

time = 27.9 min. ^{1}H NMR (400 MHz, DMSO-d_6) δ 10.63 (s, 1H), 10.53 (t, J = 5.8 Hz, 1H), 8.84

24

(s, 1H), 8.82 (s, 1H), 8.01 (d, J = 7.7 Hz, 1H), 7.41 (d, J = 15.8 Hz, 1H), 7.37-7.33 (m, 1H), 7.20-7.15 (m, 1H), 7.00 (td, J = 8.6, 2.3 Hz, 1H), 6.66 (d, J = 15.9 Hz, 1H), 4.46 (d, J = 5.7 Hz, 2H), 3.91 (td, J = 13.3, 6.6 Hz, 1H), 1.05 (d, J = 6.6 Hz, 6H). ESI-MS m/z: 458.2 (MH$^+$). HRMS calcd $C_{22}H_{22}F_2N_5O_4$ [MH$^+$], 458.1634; found, 458.1628**.**

4-Amino-N-(2,4-difluorobenzyl)-1-hydroxy-6-(3-((2-hydroxyethyl)amino)-3-oxopropyl)-2-oxo-1,2-dihydro-1,8-naphthyridine-3-carboxamide (6n) and (E)-4-Amino-N-(2,4-difluorobenzyl)-1-hydroxy-6-(3-((2-hydroxyethyl)amino)-3-oxoprop-1-en-1-yl)-2-oxo-1,2-dihydro-1,8-naphthyridine-3-carboxamide (6o). Treatment of **18g** as outlined in general procedure I and H and purification by preparative HPLC (with a linear gradient of 20% B to 50% B over 30 min) provided **6n** and **6o** as white fluffy solids. For **6n**: retention time = 22.1 min). ^{1}H NMR (400 MHz, DMSO-d_6) δ 8.56 (d, J = 1.9 Hz, 1H), 8.49 (d, J = 1.8 Hz, 1H), 7.42 (dd, J = 15.4, 8.6 Hz, 1H), 7.25-7.19 (m, 1H), 7.06 (dd, J = 9.4, 7.7 Hz, 1H), 4.50 (s, 2H), 3.32 (t, J = 6.1 Hz, 2H), 3.08 (t, J = 6.1 Hz, 2H), 2.92 (t, J = 7.5 Hz, 2H), 2.48 (t, J = 7.5 Hz, 2H). ESI-MS m/z: 462.1 (MH$^+$), 484.1 (MNa$^+$). HRMS calcd $C_{21}H_{22}F_2N_5O_5$ [MH$^+$], 462.1584; found, 462.1562**.** For **6o:** retention time = 23.9 min. ^{1}H NMR (400 MHz, DMSO-d_6) δ 10.63 (s, 1H), 10.53 (t, J = 5.8 Hz, 1H), 8.85 (s, 1H), 8.83 (s, 1H), 8.09 (t, J = 5.8 Hz, 1H), 7.43 (d, J = 15.8 Hz, 1H), 7.36 (dd, J = 15.4, 8.6 Hz, 1H), 7.20-7.15 (m, 1H), 7.03-6.98 (m, 1H), 6.73 (d, J = 15.9 Hz, 1H), 4.65 (brs, 1H), 4.46 (d, J = 5.6 Hz, 2H), 3.40 (brs, 2H), 3.20 (dd, J = 11.9, 6.0 Hz, 2H). ESI-MS m/z: 460.1 (MH$^+$), 482.1 (MNa$^+$). HRMS calcd $C_{21}H_{20}F_2N_5O_5$ [MH$^+$], 460.1427; found, 460.1421**.**

Methyl 3-(5-Amino-6-((2,4-difluorobenzyl)carbamoyl)-8-hydroxy-7-oxo-7,8-dihydro-1,8-naphthyridin-3-yl)propanoate (6p). Treatment of **19g** as outlined in

25

general procedure I and purification by preparative HPLC (linear gradient of 30 % B to 65%

B over 30 min; retention time = 23.4 min) provided **6p** as a white fluffy solid (72% yield).

^{1}H NMR (500 MHz, DMSO-d_6) δ 10.68 (t, J = 5.8 Hz, 1H), 8.62 (d, J = 1.4 Hz, 1H), 8.58 (s, 1H),

7.42 (dd, J = 15.3, 8.6 Hz, 1H), 7.26 – 7.22 (m, 1H), 7.07 (t, J = 8.5 Hz, 1H), 4.51 (d, J = 5.8 Hz,

2H), 3.58 (s, 3H), 2.95 (t, J = 7.5 Hz, 2H), 2.77 (t, J = 7.6 Hz, 2H). ESI-MS m/z: 433.1 (MH$^+$).

HRMS calcd $C_{20}H_{19}F_2N_4O_5$ [MH$^+$], 433.1318; found, 433.1311.

Methyl 2-((3-((2,4-Difluorobenzyl)carbamoyl)-1-hydroxy-6-(5-

hydroxypentyl)-2-oxo-1,2-dihydro-1,8-naphthyridin-4-yl)amino)acetate (6q).

Treatment of **18i** as outlined in general procedure I and purification by preparative HPLC

(linear gradient of 30% B to 60% B over 30 min; retention time = 20.5 min) provided **6q** as

a white fluffy solid (82% yield). ^{1}H NMR (500 MHz, DMSO-d_6) δ 10.22 (bs, 1H), 10.05 (bs,

1H), 8.48 (s, 1H), 8.22 (s, 1H), 7.52 (dd, J = 15.6, 8.6 Hz, 1H), 7.24 – 7.11 (m, 1H), 7.00 (t, J =

8.5 Hz, 1H), 4.41 (t, J = 5.5 Hz, 4H), 3.59 (s, 3H), 3.32 (t, J = 6.5 Hz, 4H), 2.62 (t, J = 7.6 Hz,

2H), 1.61 – 1.47 (m, 2H), 1.45 – 1.33 (m, 2H), 1.32 – 1.18 (m, 2H). ESI-MS m/z: 505.2 (MH$^+$).

HRMS calcd $C_{24}H_{27}F_2N_4O_6$ [MH$^+$], 505.1893; found, 505.1889.

***N*-(2,4-Difluorobenzyl)-1-hydroxy-4-((2-hydroxyethyl)amino)-6-(5-**

hydroxypentyl)-2-oxo-1,2-dihydro-1,8-naphthyridine-3-carboxamide (6r). Treatment

of **18j** as outlined in general procedure I and purification by preparative HPLC (linear

gradient of 25% B to 40% B over 30 min; retention time = 24.5 min) provided **6r** as a white

fluffy solid (22% yield). ^{1}H NMR (500 MHz, DMSO-d_6) δ 10.98 (s, 1H), 10.52 (s, 1H), 8.54 (s,

1H), 8.37 (s, 1H), 7.50 – 7.47 (m, 1H), 7.24 (t, J = 10.0 Hz, 1H), 7.07 (t, J = 8.4 Hz, 1H), 4.50 (d,

J = 5.6 Hz, 2H), 3.70 (bs, 2H), 3.61 (bs, 2H), 3.38 (t, J = 6.5 Hz, 2H), 2.69 (t, J = 7.4 Hz, 2H),

26

1.63 – 1.60 (m, 2H), 1.46 – 1.44 (m, 2H), 1.33- 1.24 (m, 2H). ESI-MS m/z: 477.2 (MH$^+$).

HRMS calcd $C_{23}H_{26}F_2N_4O_5$ [MH$^+$], 477.1944; found, 477.1944.

5-(6-((2,4-Difluorobenzyl)carbamoyl)-8-hydroxy-5-((2-hydroxyethyl)amino)-7-oxo-7,8-dihydro-1,8-naphthyridin-3-yl)pentyl Acetate (6s). The mixture of **18j** (74 mg, 0.13 mmol), triethylamine (109 μL, 0.79 mmol) and acetic anhydride (37 μl, 0.40 mmol) in CH_2Cl_2 (3 mL) was stirred at room temperature (3 h). The crude mixture was purified by silica gel chromatography to provide 5-(8-(benzyloxy)-6-((2,4-difluorobenzyl)carbamoyl)-5-((2-hydroxyethyl)amino)-7-oxo-7,8-dihydro-1,8-naphthyridin-3-yl)pent-4-yn-1-yl acetate as a colorless oil (31 mg, 39% yield). [^{1}H NMR (500 MHz, CDCl$_3$) δ 12.00 (brs, 1H), 10.69 (t, J = 5.6 Hz, 1H), 8.31 (s, 1H), 7.67 (d, J = 6.9 Hz, 2H), 7.41 – 7.36 (m, 4H), 6.86 – 6.80 (m, 2H), 5.24 (s, 2H), 4.62 (d, J = 5.6 Hz, 2H), 4.35 (t, J = 5.4 Hz, 2H), 3.94 (dd, J = 10.6, 5.3 Hz, 2H), 3.83 (t, J = 5.9 Hz, 2H), 2.60 (t, J = 7.0 Hz, 2H), 2.11 (s, 3H), 1.90 (p, J = 6.5 Hz, 2H). ESI-MS m/z: 605.2 (MH$^+$).] This compound was treated as outlined in general procedure I and purifide by preparative HPLC (linear gradient of 30% B to 55% B over 30 min; retention time = 24.1 min) to provide **6s** as a white fluffy solid (12% yield, two steps from **18j**). ^{1}H NMR (500 MHz, DMSO-d_6) δ 10.56 (brs, 1H), 10.29 (brs, 1H), 8.53 (s, 1H), 8.30 (s, 1H), 7.53 – 7.48 (m, 1H), 7.22 (t, J = 9.9 Hz, 1H), 7.07 – 7.03 (m, 1H), 4.48 (d, J = 5.8 Hz, 2H), 4.17 – 4.15 (m, 2H), 3.81 (d, J = 4.5 Hz, 2H), 3.38 – 3.36 (m, 2H), 2.68 (t, J = 7.4 Hz, 2H), 1.97 (s, 3H), 1.64 – 1.57 (m, 2H), 1.47 – 1.41 (m, 2H), 1.33 – 1.29 (m, 2H). ESI-MS m/z: 519.2 (MH$^+$), 541.1 (MNa$^+$).

Methyl 3-(6-((2,4-Difluorobenzyl)carbamoyl)-8-hydroxy-5-((2-hydroxyethyl)amino)-7-oxo-7,8-dihydro-1,8-naphthyridin-3-yl)propanoate (6t).

Treatment of **18k** as outlined in general procedure I and purification by preparative HPLC (linear gradient of 30% B to 50% B over 30 min; retention time = 21.0 min) provided **6t** as a white fluffy solid (20% yield). ^{1}H NMR (500 MHz, DMSO-d_6) δ 11.09 (bs, 1H), 10.54 (t, J = 5.7 Hz, 1H), 8.57 (d, J = 1.8 Hz, 1H), 8.43 (d, J = 1.7 Hz, 1H), 7.46 (dd, J = 15.4, 8.6 Hz, 1H), 7.26 – 7.21 (m, 1H), 7.09 – 7.05 (m, 1H), 4.50 (d, J = 5.7 Hz, 2H), 3.71 (s, 2H), 3.61 (t, J = 5.1 Hz, 2H), 3.58 (s, 3H), 2.96 (t, J = 7.4 Hz, 2H), 2.73 (t, J = 7.4 Hz, 2H). ESI-MS m/z: 477.1 (MH+). HRMS calcd $C_{23}H_{26}F_2N_4O_5$ [MH+], 477.1580; found, 477.1581.

Methyl 2-Chloro-6-methoxynicotinate (8). Commercial available 2,6-Dichloronicotinic acid **7** (3.1 g, 16 mmol) was added to the mixture of potassium t-butoxide (5.7 g, 48 mmol) in methanol (75 mL). The reaction mixture was stirred (65 °C, 24 h). The reaction mixture was concentrated and acidified using concentrated aqueous HCl. The crude mixture was filtered. The formed solid was collected to provide 2-chloro-6-methoxynicotinic acid as a white solid (2.8 g, 94% yield).[36] [^{1}H NMR (400 MHz, DMSO-d_6) δ 13.33 (bs, 1H), 8.19 (d, J = 8.5 Hz, 1H), 6.92 (d, J = 8.5 Hz, 1H), 3.92 (s, 3H). ^{13}C NMR (101 MHz, DMSO-d_6) δ 165.52, 164.54, 147.69, 143.80, 120.02, 109.82, 54.86. ESI-MS m/z: 188.0 (MH+).] 2-Chloro-6-methoxynicotinic acid (2.8 g, 15 mmol) was suspended in thionyl chloride (20 mL). The suspension was stirred and refluxed (3 h). The reaction mixture was concentrated. The residue was mixed with methanol (20 mL). The mixture was refluxed (3 h) and concentrated. The crude residue was purified by silica gel chromatography to provide **8** as a colorless oil (2.5 g, 81% yield). ^{1}H NMR (400 MHz, CDCl$_3$) δ 7.89 (d, J = 8.5 Hz, 1H), 6.48 (d, J = 8.5 Hz, 1H), 3.77 (s, 3H), 3.70 (s, 3H). ^{13}C NMR (101 MHz, CDCl$_3$) δ 164.56, 164.25, 148.96, 142.60, 118.11, 108.96, 54.30, 52.09.

28

General Procedure A for the Synthesis of Methyl 2-((Benzyloxy)amino)-nicotinates (9 and 10a). 2-Chloronicotinates (**7** and **8**) (12 mmol) were mixed with *O*-benzylhydroxylamine (48 mmol) and DIEA (36 mmol). The reaction mixture was stirred (110 °C, 18 h). The crude mixture was purified by silica gel chromatography to provide methyl 2-((benzyloxy)amino)-nicotinates (**9** and **10a**).

Methyl 2-((Benzyloxy)amino)-6-chloronicotinate (9). Treatment of methyl 2,6-dichloronicotinate, [which was prepared from commercially available 2,6-dichloronicotinic acid **7** in 91% yield based on known method.[42] ^{1}H NMR (400 MHz, CDCl$_3$) δ 8.10 (d, *J* = 8.1 Hz, 1H), 7.31 (d, *J* = 8.1 Hz, 1H), 3.90 (s, 3H). ^{13}C NMR (101 MHz, CDCl$_3$) δ 163.95, 152.88, 149.74, 142.46, 125.12, 122.79, 52.94.], as outlined in general procedure A provided **9** as a colorless oil (55% yield). ^{1}H NMR (400 MHz, CDCl$_3$) δ 10.08 (s, 1H), 8.07 – 7.97 (m, 1H), 7.52 – 7.46 (m, 2H), 7.41 – 7.25 (m, 3H), 6.77 – 6.68 (m, 1H), 5.03 (s, 2H), 3.80 (s, 3H). ^{13}C NMR (101 MHz, CDCl$_3$) δ 166.13, 159.29, 155.57, 142.02, 135.92, 129.17(2C), 128.45(3C), 114.10, 104.88, 78.29, 52.26. ESI-MS *m/z*: 293.1 (MH$^+$).

Methyl 2-((Benzyloxy)amino)-6-methoxynicotinate (10a). Treatment of **8** as outlined in general procedure A provided **10a** as a colorless oil (51% yield). ^{1}H NMR (400 MHz, CDCl$_3$) δ 10.22 (s, 1H), 7.99 (d, *J* = 8.6 Hz, 1H), 7.47 – 7.45 (m, 2H), 7.38 – 7.29 (m, 3H), 6.16 (d, *J* = 8.6 Hz, 1H), 5.09 (s, 2H), 3.99 (s, 3H), 3.78 (s, 3H). ^{13}C NMR (101 MHz, CDCl$_3$) δ 166.82, 166.70, 160.47, 142.09, 136.36, 128.81 (2C), 128.42 (2C), 128.26, 101.26, 98.90, 78.39, 53.74, 51.67.

General Procedure B for the Synthesis of 6-Substituted Methyl 2-((Benzyloxy)amino)-nicotinates (10b and 10c). Methyl 2-((benzyloxy)amino)-6-chloronicotinate (**9**) (1 mmol) was dissolved in DMF (1 mL). Piperidine or morphiline (4

mmol) was added. The mixture was stirred and heated (80 °C, 1 h). The crude mixture was

purified by silica gel chromatography to provide 6-substituted methyl 2-

((benzyloxy)amino)-nicotinates (**10b** and **10c**).

Methyl 2-((Benzyloxy)amino)-6-(piperidin-1-yl)nicotinate (10b). Treatment of

9 with piperidine as outlined in general procedure B provided **10b** as a colorless oil (88%

yield). ^{1}H NMR (400 MHz, CDCl$_3$) δ 10.12 (s, 1H), 7.85 (dd, J = 9.0, 0.7 Hz, 1H), 7.46 – 7.44

(m, 2H), 7.36 – 7.30 (m, 4H), 6.05 (d, J = 9.0 Hz, 1H), 5.07 (s, 2H), 3.74 (d, J = 0.7 Hz, 3H),

3.39 – 3.66 (m, 4H), 1.67 – 1.65 (m, 2H), 1.63 – 1.61 (m, 4H). ^{13}C NMR (101 MHz, CDCl$_3$) δ

166.99, 160.55, 159.92, 140.74, 136.79, 128.74 (2C), 128.60, 128.42, 128.33 (2C), 128.05,

97.10, 94.46, 78.11, 51.22, 45.70, 25.66, 24.74. ESI-MS m/z: 342.2 (MH$^+$).

Methyl 2-((Benzyloxy)amino)-6-morpholinonicotinate (10c). Treatment of **9**

with morpholine as outlined in general procedure B provided **10c** as a colorless oil (99%

yield). ^{1}H NMR (400 MHz, CDCl$_3$) δ 10.13 (s, 1H), 7.88 (d, J = 8.8 Hz, 1H), 7.41 (dd, J = 8.0,

1.5 Hz, 2H), 7.34 – 7.23 (m, 3H), 5.99 (d, J = 8.9 Hz, 1H), 5.03 (s, 2H), 3.73 (s, 3H), 3.73 –

3.71 (m, 4H), 3.63 – 3.60 (m, 4H). ^{13}C NMR (101 MHz, CDCl$_3$) δ 166.86, 160.19 (2C), 141.05,

136.70, 128.63 (2C), 128.36 (2C), 128.11, 96.84, 95.76, 78.11, 66.57 (2C), 51.36, 44.73 (2C).

ESI-MS m/z: 344.2 (MH$^+$).

General Procedure C for the Synthesis of Methyl Nicotinates (11a–c). Methyl 3-

chloro-3-oxopropanoate (12 mmol) was added dropwise to a solution of methyl 2-

((benzyloxy)amino)-nicotinates (**10a–c**) (6 mmol) and triethylamine (12 mmol) in CH$_2$Cl$_2$

(40 mL). The mixture was stirred at room temperature (1 h). The crude mixture was

filtered and the filtrate was concentrated. The crude residue was purified by silica gel

chromatography to provide methyl nicotinates (**11a–c**).

30

Methyl 2-(*N*-(Benzyloxy)-3-methoxy-3-oxopropanamido)-6-(piperidin-1-yl)nicotinate (11b). Treatment of **10b** as outlined in general procedure C provided **11b** as a yellow oil (76% yield). ^{1}H NMR (400 MHz, CDCl$_3$) δ 7.93 (d, *J* = 8.9 Hz, 1H), 7.30 (d, *J* = 3.8 Hz, 2H), 7.24 – 7.23 (m, 3H), 6.49 (d, *J* = 9.0 Hz, 1H), 4.99 (s, 2H), 3.90 (s, 1H), 3.80 (s, 1H), 3.72 (s, 3H), 3.62 (s, 3H), 3.55-3.56 (m, 4H), 1.61 – 1.58 (m, 2H), 1.55-1.54 (m, 4H). ESI-MS *m/z*: 442.2 (MH$^+$).

Methyl 2-(*N*-(Benzyloxy)-3-methoxy-3-oxopropanamido)-6-morpholinonicotinate (11c). Treatment of **10c** as outlined in general procedure C provided **11c** as a yellow oil (79% yield). ^{1}H NMR (400 MHz, CDCl$_3$) δ 8.04 (d, *J* = 8.8 Hz, 1H), 7.32-7.28 (m, 5H), 6.52 (dd, *J* = 8.9, 0.9 Hz, 1H), 5.01 (s, 2H), 3.85-3.83 (m, 1H), 3.78 (s, 3H), 3.77-3.75 (m, 4H), 3.72 – 3.71 (m, 1H), 3.68 (s, 3H), 3.60-3.57 (m, 4H). ESI-MS *m/z*: 444.2 (MH$^+$).

General Procedure D for the Synthesis of Methyl Carboxylates (12a–c). A solution of sodium methanolate (16 mmol, 25% in methanol) was added to a solution of methyl nicotinates (**11a–c**) (6 mmol) in methanol (4 mL). The mixture was stirred at room temperature (18 h). The reaction mixture was brought to pH 4 by the addition of aqueous HCl (2N) and stirred (0 °C, 15 min). The crude suspension was filtered and the solid was collected to provide methyl carboxylates (**12a–c**).

Methyl 1-(Benzyloxy)-4-hydroxy-7-methoxy-2-oxo-1,2-dihydro-1,8-naphthyridine-3-carboxylate (12a). Treatment of **10a** as outlined in general procedure C and D provided **12a** as a white solid (54% yield, two steps). ^{1}H NMR (400 MHz, CDCl$_3$) δ 8.20 (d, *J* = 8.7 Hz, 1H), 7.62 – 7.59 (m, 2H), 7.35 – 7.32 (m, 3H), 6.61 (d, *J* = 8.7 Hz, 1H), 5.21 (s, 2H), 4.05 (s, 3H), 4.00 (s, 3H). ^{13}C NMR (101 MHz, CDCl$_3$) δ 172.60, 170.32, 167.69,

31

156.93, 149.75, 136.69, 134.30, 129.68 (2C), 128.94, 128.42 (2C), 107.37, 102.64, 96.48,

77.90, 54.52, 53.01.

Methyl 1-(Benzyloxy)-4-hydroxy-2-oxo-7-(piperidin-1-yl)-1,2-dihydro-1,8-naphthyridine-3-carboxylate (12b). Treatment of **11b** as outlined in general procedure

D provided **12b** as a white solid in 62% yield. ^{1}H NMR (400 MHz, CDCl$_3$) δ 13.91 (s, 1H),

8.00 (d, J = 9.1 Hz, 1H), 7.61 (dd, J = 7.4, 1.7 Hz, 2H), 7.34 (d, J = 7.0 Hz, 3H), 6.49 (d, J = 9.1

Hz, 1H), 5.18 (s, 2H), 3.98 (s, 3H), 3.75 – 3.73 (m, 4H), 1.71-1.70 (m, 2H), 1.65 – 1.63 (m,

4H). ^{13}C NMR (101 MHz, CDCl$_3$) δ 172.95, 170.00, 160.00, 157.59, 150.44, 135.06, 134.75,

129.66(2C), 128.71, 128.33(2C), 102.62, 98.44, 94.11, 77.47 (2C), 52.65, 46.08, 25.76(2C),

24.56. ESI-MS m/z: 410.2 (MH$^+$).

Methyl 1-(Benzyloxy)-4-hydroxy-7-morpholino-2-oxo-1,2-dihydro-1,8-naphthyridine-3-carboxylate (12c). Treatment of **11c** as outlined in general procedure D

provided **12c** as a white solid (84% yield). ^{1}H NMR (400 MHz, DMSO-d_6) δ 7.97 (d, J = 9.3

Hz, 1H), 7.53-7.51 (m, 2H), 7.39-7.33 (m, 4H), 6.60 (d, J = 9.3 Hz, 1H), 5.00 (s, 2H), 3.72-3.54

(m, 11H). ESI-MS m/z: 412.2 (MH$^+$).

General Procedure E for the Synthesis of Carboxyamides (13a−c). A solution of

methyl carboxylates (**12a−c**) (0.3 mmol) and (2,4-difluorophenyl)methanamine (1.5 mmol)

in DMF (1 mL) was heated (140 °C, 2 h) in microwave reactor. The crude mixture was

purified by silica gel chromatography and recrystallized from methanol to provide

carboxamides (**13a−c**).

1-(Benzyloxy)-N-(2,4-difluorobenzyl)-4-hydroxy-7-methoxy-2-oxo-1,2-dihydro-1,8-naphthyridine-3-carboxamide (13a). Treatment of **12a** as outlined in

32

general procedure E provided **13a** as a white solid (45% yield). ^{1}H NMR (400 MHz, CDCl$_3$) δ

10.24 (t, J = 5.6 Hz, 1H), 8.22 (dd, J = 8.7, 0.4 Hz, 1H), 7.56 – 7.53 (m, 2H), 7.35 – 7.29 (m,

4H), 6.81 – 6.73 (m, 2H), 6.62 (dd, J = 8.7, 0.4 Hz, 1H), 5.20 (d, J = 0.6 Hz, 2H), 4.58 (d, J = 6.0

Hz, 2H), 4.02 (d, J = 0.5 Hz, 3H). ESI-MS m/z: 468.2 (MH$^+$).

1-(Benzyloxy)-*N*-(2,4-difluorobenzyl)-4-hydroxy-2-oxo-7-(piperidin-1-yl)-1,2-

dihydro-1,8-naphthyridine-3-carboxamide (13b). Treatment of **12b** as outlined in

general procedure E provided **13b** as a white solid (90% yield). ^{1}H NMR (400 MHz, CDCl$_3$) δ

10.30 (t, J = 6.0 Hz, 1H), 10.03 (s, 1H), 8.05 (dd, J = 9.1, 0.7 Hz, 1H), 7.58 – 7.56 (m, 2H), 7.38

– 7.33 (m, 4H), 6.85 – 6.76 (m, 2H), 6.54 (dd, J = 9.1, 0.7 Hz, 1H), 5.20 (s, 2H), 4.60 (d, J = 6.0

Hz, 2H), 3.76-3.74 (m, 4H), 1.71 – 1.69 (m, 2H), 1.67-1.61 (m, 4H). ESI-MS m/z: 521.2 (MH$^+$).

1-(Benzyloxy)-*N*-(2,4-difluorobenzyl)-4-hydroxy-7-morpholino-2-oxo-1,2-

dihydro-1,8-naphthyridine-3-carboxamide (13c). Treatment of **12c** as outlined in

general procedure E provided **13c** as a white solid (89% yield). ^{1}H NMR (400 MHz, CDCl$_3$) δ

10.22 (bs, 1H), 8.08 (d, J = 9.1 Hz, 1H), 7.50-7.48 (m, 2H), 7.33 – 7.24 (m, 4H), 6.79 – 6.69

(m, 2H), 6.48 (d, J = 9.1 Hz, 1H), 5.15 (s, 2H), 4.56 (d, J = 6.2 Hz, 2H), 3.73 – 3.66 (m, 8H).

ESI-MS m/z: 523.2 (MH$^+$).

General Procedure F for the Synthesis of *p*-Methylbenzenesulfonates (14a−c).

Compound 4-hydroxyl analogues (**13a−c**) (0.5 mmol) were dissolved in CH$_3$CN (3 mL).

DIEA (2.8 mmol), CH$_2$Cl$_2$ (2 mL) and *p*-methylbenzene-1-sulfonyl chloride (1.4 mmol) were

added. The reaction mixture was stirred at room temperature (18 h). The mixture crude

was purified by silica gel chromatography to provide *p*-methylbenzenesulfonates (**14a−c**).

33

1-(Benzyloxy)-3-((2,4-difluorobenzyl)carbamoyl)-7-methoxy-2-oxo-1,2-dihydro-1,8-naphthyridin-4-yl 4-Methylbenzenesulfonate (14a). Treatment of **13a** as outlined in general procedure F provided **14a** as a colorless oil (68% yield). ^{1}H NMR (400 MHz, CDCl$_3$) δ 8.53 (t, J = 5.9 Hz, 1H), 8.01 (d, J = 8.8 Hz, 1H), 7.87 (d, J = 8.3 Hz, 2H), 7.58 – 7.56 (m, 2H), 7.46 – 7.44 (m, 1H), 7.37 – 7.35 (m, 3H), 7.32 (dd, J = 8.6, 0.7 Hz, 2H), 6.83 – 6.74 (m, 2H), 6.64 (d, J = 8.8 Hz, 1H), 5.25 (s, 2H), 4.48 – 4.46 (m, 2H), 4.06 (s, 3H), 2.43 (s, 3H). ESI-MS *m/z*: 622.1(MH+).

1-(Benzyloxy)-3-((2,4-difluorobenzyl)carbamoyl)-2-oxo-7-(piperidin-1-yl)-1,2-dihydro-1,8-naphthyridin-4-yl 4-Methylbenzenesulfonate (14b). Treatment of **13b** as outlined in general procedure F provided **14b** as a colorless oil (53% yield). ^{1}H NMR (400 MHz, CDCl$_3$) δ 8.83 (t, J = 5.9 Hz, 1H), 7.88 (dd, J = 8.8, 3.2 Hz, 3H), 7.58 – 7.55 (m, 2H), 7.44 – 7.35 (m, 4H), 7.31 – 7.29 (m, 2H), 6.82 – 6.73 (m, 2H), 6.57 (d, J = 9.3 Hz, 1H), 5.22 (s, 2H), 4.44 (s, 2H), 3.76 (bs, 4H), 2.42 (s, 3H), 1.72-1.69 (m, 2H), 1.66-1.64 (m, 4H). ESI-MS *m/z*: 675.2 (MH+).

1-(Benzyloxy)-3-((2,4-difluorobenzyl)carbamoyl)-7-morpholino-2-oxo-1,2-dihydro-1,8-naphthyridin-4-yl 4-Methylbenzenesulfonate (14c). Treatment of **13c** as outlined in general procedure F provided **14c** as a colorless oil (27% yield). ^{1}H NMR (400 MHz, CDCl$_3$) δ 8.71 (t, J = 5.9 Hz, 1H), 8.19 – 8.18 (m, 2H), 7.94 (d, J = 9.2 Hz, 1H), 7.86 (d, J = 8.4 Hz, 2H), 7.36 – 7.50 (m, 2H), 7.36 – 7.28 (m, 3H), 6.82 – 6.74 (m, 3H), 6.55 (dd, J = 9.2, 0.7 Hz, 1H), 5.21 (s, 2H), 4.43-4.41 (m, 2H), 3.78 – 3.73 (m, 8H), 2.42 (s, 3H). ESI-MS *m/z*: 677.2 (MH+).

34

1
2
3
4
5
6
7
8
9
10
11
12
13
14
15
16
17
18
19
20
21
22
23
24
25
26
27
28
29
30
31
32
33
34
35
36
37
38
39
40
41
42
43
44
45
46
47
48
49
50
51
52
53
54
55
56
57
58
59
60

General Procedure G for the Synthesis of 4-Substituted Amines (15a–f, 17d and 17e). A solution of *p*-methylbenzenesulfonates (**14a–c** and **17b**) (0.2 mmol), DIPEA (2 mmol) and methyl 2-aminoacetate hydrochloride or 2,4-dimethoxyphenyl)methanamine (1 mmol) in DMF (2 mL) was stirred and heated (50 °C, 1 h). The crude mixture was purified by silica gel chromatography to provide 4-substituted amines (**15a–f**, **17d** and **17e**).

Methyl 2-((1-(Benzyloxy)-3-((2,4-difluorobenzyl)carbamoyl)-7-methoxy-2-oxo-1,2-dihydro-1,8-naphthyridin-4-yl)amino)acetate (15a). Treatment of **14a** with methyl 2-aminoacetate hydrochloride as outlined in general procedure G provided **15a** as a white solid (91% yield). ^{1}H NMR (400 MHz, CDCl$_3$) δ 12.20 (t, J = 5.5 Hz, 1H), 10.70 (t, J = 5.7 Hz, 1H), 8.02 (d, J = 8.9 Hz, 1H), 7.59 – 7.56 (m, 2H), 7.41 – 7.32 (m, 4H), 6.82 – 6.74 (m, 2H), 6.55 (d, J = 8.9 Hz, 1H), 5.20 (s, 2H), 4.61 (d, J = 5.8 Hz, 2H), 4.35 (d, J = 5.5 Hz, 2H), 4.02 (s, 3H), 3.76 (s, 3H). ESI-MS *m/z*: 539.2 (MH$^+$).

Methyl 2-((1-(Benzyloxy)-3-((2,4-difluorobenzyl)carbamoyl)-2-oxo-7-(piperidin-1-yl)-1,2-dihydro-1,8-naphthyridin-4-yl)amino)acetate (15b). Treatment of **14b** with methyl 2-aminoacetate hydrochloride as outlined in general procedure G provided **15b** as a white solid (80% yield). ^{1}H NMR (400 MHz, CDCl$_3$) δ 11.99 (t, J = 5.7 Hz, 1H), 10.78 (t, J = 5.8 Hz, 1H), 7.81 (d, J = 9.3 Hz, 1H), 7.58 – 7.55 (m, 2H), 7.41 – 7.31 (m, 4H), 6.81 – 6.72 (m, 2H), 6.40 (d, J = 9.3 Hz, 1H), 5.18 (s, 2H), 4.60 (d, J = 5.7 Hz, 2H), 4.32 (d, J = 5.6 Hz, 2H), 3.76 (s, 3H), 3.71 – 3.69 (m, 4H), 1.71-1.67 (m, 2H), 1.64-1.59 (m, 4H). ESI-MS *m/z*: 592.2 (MH$^+$).

Methyl 2-((1-(Benzyloxy)-3-((2,4-difluorobenzyl)carbamoyl)-7-morpholino-2-oxo-1,2-dihydro-1,8-naphthyridin-4-yl)amino)acetate (15c). Treatment of **14c** with

methyl 2-aminoacetate hydrochloride as outlined in general procedure G provided **15c** as a white solid (63% yield). ^{1}H NMR (400 MHz, CDCl$_3$) δ 12.06 (t, J = 5.6 Hz, 1H), 10.73 (t, J = 5.8 Hz, 1H), 7.88 (dd, J = 9.2, 0.8 Hz, 1H), 7.53 – 7.50 (m, 2H), 7.41 – 7.27 (m, 3H), 6.81-6.73 (m, 3H), 6.38 (dd, J = 9.3, 0.8 Hz, 1H), 5.16 (s, 2H), 4.60 (d, J = 5.8 Hz, 2H), 4.32 (d, J = 5.5 Hz, 2H), 3.76 (s, 3H), 3.75 – 3.73 (m, 4H), 3.68-3.65 (m, 4H). ESI-MS m/z: 594.2 (MH$^+$).

1-(Benzyloxy)-*N*-(2,4-difluorobenzyl)-4-((2,4-dimethoxybenzyl)amino)-7-methoxy-2-oxo-1,2-dihydro-1,8-naphthyridine-3-carboxamide (15d). Treatment of **14a** with (2,4-dimethoxyphenyl)methanamine as outlined in general procedure G provided **15d** as a white solid which was directly used in next step. ^{1}H NMR (400 MHz, CDCl$_3$) δ 11.88 (t, J = 6.2 Hz, 1H), 10.77 (t, J = 5.8 Hz, 1H), 8.10 (dd, J = 8.9, 0.7 Hz, 1H), 7.61 – 7.59 (m, 2H), 7.38 – 7.31 (m, 4H), 7.24 – 7.21 (m, 1H), 6.81 – 6.73 (m, 2H), 6.47 – 6.42 (m, 3H), 5.24 (s, 2H), 4.67 (d, J = 6.1 Hz, 2H), 4.56 (d, J = 5.7 Hz, 2H), 4.02 (s, 3H), 3.77 (s, 3H), 3.75 (s, 3H). ESI-MS m/z: 617.2 (MH$^+$).

1-(Benzyloxy)-*N*-(2,4-difluorobenzyl)-4-((2,4-dimethoxybenzyl)amino)-2-oxo-7-(piperidin-1-yl)-1,2-dihydro-1,8-naphthyridine-3-carboxamide (15e). Treatment of **14b** with (2,4-dimethoxyphenyl)methanamine as outlined in general procedure G provided **15e** as a white solid (65% yield). ^{1}H NMR (400 MHz, CDCl$_3$) δ 11.71 (t, J = 6.2 Hz, 1H), 10.85 (t, J = 5.8 Hz, 1H), 7.88 (d, J = 9.3 Hz, 1H), 7.60-7.57 (m, 2H), 7.37 – 7.32 (m, 4H), 7.27 – 7.24 (m, 1H), 6.81 – 6.72 (m, 2H), 6.44 – 6.42 (m, 2H), 6.30 (d, J = 9.3 Hz, 1H), 5.20 (s, 2H), 4.64 (d, J = 6.2 Hz, 2H), 4.55 (d, J = 6.1 Hz, 2H), 3.77 (s, 3H), 3.76 (s, 3H), 3.70-3.67 (m, 4H), 1.70 – 1.66 (m, 2H), 1.63 – 1.58 (m, 4H). ESI-MS m/z: 670.3 (MH$^+$).

1-(Benzyloxy)-*N*-(2,4-difluorobenzyl)-4-((2,4-dimethoxybenzyl)amino)-7-morpholino-2-oxo-1,2-dihydro-1,8-naphthyridine-3-carboxamide (15f). Treatment of

36

14c with (2,4-dimethoxyphenyl)methanamine as outlined in general procedure G provided

15f as a white solid which was directly used in next step. ^{1}H NMR (400 MHz, CDCl$_3$) δ 11.73

(t, J = 6.1 Hz, 1H), 10.75 (t, J = 5.8 Hz, 1H), 7.95 (d, J = 9.2 Hz, 1H), 7.52 – 7.50 (m, 2H), 7.33 –

7.21 (m, 5H), 6.80 – 6.71 (m, 4H), 6.30 (d, J = 9.2 Hz, 1H), 5.16 (s, 2H), 4.63 (d, J = 6.1 Hz,

2H), 4.51 (d, J = 5.8 Hz, 2H), 3.76 (s, 3H), 3.74 (s, 3H), 3.73 – 3.71 (m, 4H), 3.65-3.63 (m, 4H).

ESI-MS m/z: 672.3 (MH$^+$).

General Procedure H for the Synthesis of Amine Analogues (16a–c, 19b–g).

The 2,4-dimethoxybenzyl protected compounds (**15d–f** and **18a–h**) (0.25 mmol) were

dissolved in CH$_2$Cl$_2$ (2 mL). TFA (2 mL) was added at room temperature. The reaction

mixture was concentrated. The crude residue was purified by silica gel chromatography to

provide amine analogues (**16a–c** and **19b–g**).

4-Amino-1-(benzyloxy)-*N*-(2,4-difluorobenzyl)-7-methoxy-2-oxo-1,2-dihydro-

1,8-naphthyridine-3-carboxamide (16a). Treatment of **15d** as outlined in general

procedure H provided **16a** as a colorless oil (72% yield, two steps (general procedures G

and H). ^{1}H NMR (400 MHz, CDCl$_3$) δ 10.60 (t, J = 5.9 Hz, 1H), 7.85 (dd, J = 8.7, 0.7 Hz, 1H),

7.58 (dd, J = 7.3, 2.2 Hz, 2H), 7.36 – 7.32 (m, 4H), 6.81 – 6.74 (m, 2H), 6.58 (dd, J = 8.8, 0.7

Hz, 1H), 5.21 (s, 2H), 4.58 (d, J = 5.8 Hz, 2H), 4.03 (s, 3H). ESI-MS m/z: 467.2 (MH$^+$).

4-Amino-1-(benzyloxy)-*N*-(2,4-difluorobenzyl)-2-oxo-7-(piperidin-1-yl)-1,2-

dihydro-1,8-naphthyridine-3-carboxamide (16b). Treatment of **15e** as outlined in

general procedure H provided **16b** as a colorless oil (46% yield, two steps (general

procedures G and H). ^{1}H NMR (400 MHz, CDCl$_3$) δ 10.62 (t, J = 5.9 Hz, 1H), 7.58 (d, J = 9.1 Hz,

1H), 7.54 – 7.52 (m, 2H), 7.35 – 7.26 (m, 4H), 6.78 – 6.69 (m, 2H), 6.44 (d, J = 9.2 Hz, 1H),

37

5.15 (s, 2H), 4.54 (d, J = 5.8 Hz, 2H), 3.70 – 3.65 (m, 4H), 1.66 – 1.63 (m, 2H), 1.61-1.57 (m, 4H). ESI-MS m/z: 520.2 (MH[+]).

4-Amino-1-(benzyloxy)-N-(2,4-difluorobenzyl)-7-morpholino-2-oxo-1,2-dihydro-1,8-naphthyridine-3-carboxamide (16c). Treatment of **15f** as outlined in general procedure H provided **16c** as a colorless oil (32% yield, two steps (general procedures G and H). ^{1}H NMR (400 MHz, CDCl3) δ 10.61 (t, J = 5.7 Hz, 1H), 7.70 (d, J = 9.0 Hz, 1H), 7.57 – 7.49 (m, 2H), 7.41 – 7.28 (m, 3H), 6.83 – 6.71 (m, 3H), 6.48 (dd, J = 9.1, 0.7 Hz, 1H),5.18 (s, 2H), 4.58 (d, J = 5.8 Hz, 2H), 3.81 – 3.75 (m, 4H), 3.69-3.67 (m, 4H). ESI-MS m/z: 522.2 (MH[+]).

Methyl 2-((1-(Benzyloxy)-6-bromo-3-((2,4-difluorobenzyl)carbamoyl)-2-oxo-1,2-dihydro-1,8-naphthyridin-4-yl)amino)acetate (**17d**)**.** Treatment of 1-(benzyloxy)-6-bromo-3-((2,4-difluorobenzyl)carbamoyl)-2-oxo-1,2-dihydro-1,8-naphthyridin-4-yl 4-methylbenzenesulfonate **17b**[31] with methyl glycinate as outlined in general procedure G provided **17d** as a white solid (74% yield). ^{1}H NMR (400 MHz, CDCl3) δ 12.05 (t, J = 6.2 Hz, 1H), 10.61 (t, J = 5.7 Hz, 1H), 8.58 (d, J = 2.1 Hz, 1H), 8.34 (d, J = 2.2 Hz, 1H), 7.57 (dd, J = 7.3, 1.9 Hz, 2H), 7.39 – 7.22 (m, 4H), 7.17 (dd, J = 8.9, 4.3 Hz, 1H), 6.85 – 6.63 (m, 2H), 6.47 – 6.34 (m, 2H), 5.15 (s, 2H), 4.64 (d, J = 6.3 Hz, 2H), 4.52 (d, J = 5.7 Hz, 2H), 3.74 (s, 3H), 3.73 (s, 3H). ESI-MS m/z: 587.1, 589.1 (MH[+]).

1-(Benzyloxy)-6-bromo-N-(2,4-difluorobenzyl)-4-((2-hydroxyethyl)amino)-2-oxo-1,2-dihydro-1,8-naphthyridine-3-carboxamide (**17e**)**.** Treatment of 1-(benzyloxy)-6-bromo-3-((2,4-difluorobenzyl)carbamoyl)-2-oxo-1,2-dihydro-1,8-naphthyridin-4-yl 4-methylbenzenesulfonate **17b**[31] with 2-aminoethan-1-ol as outlined in general procedure G

38

provided **17e** as a white solid (93% yield). ^{1}H NMR (500 MHz, CDCl$_3$) δ 11.65 (bs, 1H),

10.65 (bs, 1H), 8.64 (d, J = 1.9 Hz, 1H), 8.47 (d, J = 1.9 Hz, 1H), 7.58 (d, J = 6.1 Hz, 2H), 7.31 (t,

J = 7.2 Hz, 4H), 6.79 – 6.73 (m, 2H), 5.15 (s, 2H), 4.55 (d, J = 5.6 Hz, 2H), 3.88 – 3.86 (m, 2H),

3.78 – 3.75 (m, 2H). ESI-MS m/z: 559.1, 561.1 (MH$^+$).

General Procedure J for the Synthesis of 6-Alkylated Analogues (18a, 18b, 18d,

18i, and 18j) Using Sonogashira Reaction. Bromides (**17a** and **17c−e**) (0.3 mmol) were

mixed with bis(triphenylphosphine)palladium (II) dichloride (9 µmol), DIEA (0.3 mmol),

copper(I) iodide (0.03 mmol) in DMF (1.5 mL) in a reaction tube. The related terminal

alkynes (0.45 mmol) were added. The reaction mixture was flushed with argon and sealed

with cap and heated (70°C, 4 h). The crude mixture was purified by silica gel

chromatography to provide 6-alkylated analogue (**18a**, **18b**, **18d**, **18i**, and **18j**).

General Procedure K for the Synthesis of 6-Alkylated Analogues (18c, 18e−h

and 18k) Using Heck Reaction. The mixture of bromides (**17c** and **17e**) (0.2 mmol),

alkenes (0.4 mmol), triethylamine (0.6 mmol), diacetoxypalladium (0.04 mmol), and

triphenylphosphine (0.08 mmol) in DMF (0.5 mL) was flushed with argon and sealed in a

reaction tube. The reaction mixture was microwave-heated (100 °C, 5 h). The crude

mixture was purified by silica gel chromatography to provide 6-alkylated analogues (**18c**,

18e−h and **18k**).

1-(Benzyloxy)-6-(3-cyclohexylprop-1-yn-1-yl)-N-(2,4-difluorobenzyl)-4-((2,4-

dimethoxybenzyl)amino)-2-oxo-1,2-dihydro-1,8-naphthyridine-3-carboxamide

(18a). Treatment of 1-(benzyloxy)-6-bromo-N-(2,4-difluorobenzyl)-4-((2,4-

dimethoxybenzyl)amino)-2-oxo-1,2-dihydro-1,8-naphthyridine-3-carboxamide **17c**[31] with

39

commercial available prop-2-yn-1-ylcyclohexane as outlined in general procedure J

provided **18a** as a colorless oil (79% yield). ^{1}H NMR (500 MHz, CDCl$_3$) δ 12.02 (t, J = 5.8 Hz,

1H), 10.70 (t, J = 5.7 Hz, 1H), 8.66 (t, J = 1.6 Hz, 1H), 8.32 (s, 1H), 7.68 (d, J = 7.7 Hz, 2H),

7.40 – 7.36 (m, 4H), 7.25-7.24 (m, 1H), 6.85 – 6.78 (m, 2H), 6.48 – 6.45 (m, 2H), 5.25 (s, 2H),

4.75 (d, J = 6.0 Hz, 2H), 4.60 (d, J = 5.6 Hz, 2H), 3.82 (s, 3H), 3.80 (s, 3H), 2.32 (d, J = 6.6 Hz,

2H), 1.85 (d, J = 12.3 Hz, 2H), 1.78 – 1.68 (m, 3H), 1.57 (ddd, J = 10.9, 7.0, 3.6 Hz, 1H), 1.31 –

1.16 (m, 3H), 1.05 (qd, J = 12.4, 3.3 Hz, 2H).

1-(Benzyloxy)-*N*-(2,4-difluorobenzyl)-4-((2,4-dimethoxybenzyl)amino)-2-oxo-6-(4-phenylbut-1-yn-1-yl)-1,2-dihydro-1,8-naphthyridine-3-carboxamide (18b).

Treatment of 1-(benzyloxy)-6-bromo-*N*-(2,4-difluorobenzyl)-4-((2,4-dimethoxybenzyl)amino)-2-oxo-1,2-dihydro-1,8-naphthyridine-3-carboxamide **17c**[31] with

commercial available but-3-yn-1-ylbenzene as outlined in general procedure J provided

18b as a colorless oil (98% yield). ^{1}H NMR (500 MHz, CDCl$_3$) δ 11.99 (t, J = 5.6 Hz, 1H),

10.68 (t, J = 5.7 Hz, 1H), 8.62 (s, 1H), 8.31 (s, 1H), 7.68 – 7.66 (m, 2H), 7.39 – 7.31 (m, 6H),

7.27 – 7.21 (m, 4H), 6.85 – 6.77 (m, 2H), 6.47 – 6.46 (m, 2H), 5.24 (s, 2H), 4.73 (d, J = 5.8 Hz,

2H), 4.59 (d, J = 5.7 Hz, 2H), 3.81 (s, 3H), 3.76 (s, 3H), 2.92 (d, J = 7.4 Hz, 2H), 2.73 (t, J = 7.4

Hz, 2H).

(*E*)-1-(Benzyloxy)-*N*-(2,4-difluorobenzyl)-4-((2,4-dimethoxybenzyl)amino)-2-oxo-6-styryl-1,2-dihydro-1,8-naphthyridine-3-carboxamide (18c). Treatment of 1-(benzyloxy)-6-bromo-*N*-(2,4-difluorobenzyl)-4-((2,4-dimethoxybenzyl)amino)-2-oxo-1,2-dihydro-1,8-naphthyridine-3-carboxamide **17c**[31] with commercial available styrene as

outlined in general procedure K provided **18c** as a colorless oil (27% yield). ^{1}H NMR (500

40

MHz, CDCl$_3$) δ 12.14 (t, J = 6.7 Hz, 1H), 10.81 (t, J = 5.9 Hz, 1H), 8.71 (s, 1H), 8.44 (s, 1H),

7.71 (d, J = 6.7 Hz, 2H), 7.44 – 7.38 (m, 10H), 6.99 (d, J = 16.4 Hz, 1H), 6.88-6.81 (m, 2H),

6.58-6.52 (m, 3H), 5.29 (s, 2H), 4.80 (d, J = 6.7 Hz, 2H), 4.65 (d, J = 5.6 Hz, 2H), 3.86 (s, 3H),

3.77 (s, 3H).

1-(Benzyloxy)-*N*-(2,4-difluorobenzyl)-4-((2,4-dimethoxybenzyl)amino)-6-(3-(2-hydroxyethoxy)prop-1-yn-1-yl)-2-oxo-1,2-dihydro-1,8-naphthyridine-3-carboxamide (18d). Treatment of 1-(Benzyloxy)-6-bromo-*N*-(2,4-difluorobenzyl)-4-((2,4-dimethoxybenzyl)amino)-2-oxo-1,2-dihydro-1,8-naphthyridine-3-carboxamide **17c**[31] with 2-(prop-2-yn-1-yloxy)ethanol as outlined in general procedure J provided **18d** as a colorless oil (64% yield). ^{1}H NMR (500 MHz, CDCl$_3$) δ 12.06 (t, J = 5.9 Hz, 1H), 10.66 (t, J = 5.7 Hz, 1H), 8.70 (d, J = 1.2 Hz, 1H), 8.38 (d, J = 1.4 Hz, 1H), 7.67 (d, J = 6.6 Hz, 2H), 7.41 – 7.34 (m, 4H), 7.24 (d, J = 7.9 Hz, 1H), 6.85 – 6.79 (m, 2H), 6.49 – 6.43 (m, 2H), 5.25 (s, 2H), 4.75 (d, J = 6.0 Hz, 2H), 4.60 (d, J = 5.7 Hz, 2H), 4.45 (s, 2H), 3.82 (s, 3H), 3.84 – 3.81 (m, 2H), 3.80 (s, 3H), 3.71 – 3.69 (m, 2H).

(*E*)-1-(Benzyloxy)-*N*-(2,4-difluorobenzyl)-4-((2,4-dimethoxybenzyl)amino)-6-(3-(dimethylamino)-3-oxoprop-1-en-1-yl)-2-oxo-1,2-dihydro-1,8-naphthyridine-3-carboxamide (18e). Treatment of 1-(benzyloxy)-6-bromo-N-(2,4-difluorobenzyl)-4-((2,4-dimethoxybenzyl)amino)-2-oxo-1,2-dihydro-1,8-naphthyridine-3-carboxamide **17c**[31] with commercial available *N,N*-dimethylacrylamide as outlined in general procedure K provided **18e** as a colorless oil (41% yield). ^{1}H NMR (400 MHz, CDCl$_3$) δ 12.17 (t, J = 6.5 Hz, 1H), 10.74 (t, J = 5.7 Hz, 1H), 8.79 (d, J = 1.8 Hz, 1H), 8.39 (d, J = 1.8 Hz, 1H), 7.72-7.67 (m, 3H), 7.60-7.55 (m, 1H), 7.51-7.46 (m, 1H), 7.44-7.38 (m, 4H), 6.88-6.81 (m, 2H), 6.51-6.48 (m,

41

2H), 5.28 (s, 2H), 4.77 (d, J = 6.6 Hz, 2H), 4.64 (d, J = 5.7 Hz, 2H), 3.83 (s, 3H), 3.83 (s, 3H),

3.07 (s, 3H), 3.00 (s, 3H).

(*E*)-1-(Benzyloxy)-*N*-(2,4-difluorobenzyl)-4-((2,4-dimethoxybenzyl)amino)-6-(3-(isopropylamino)-3-oxoprop-1-en-1-yl)-2-oxo-1,2-dihydro-1,8-naphthyridine-3-carboxamide (18f). Treatment of 1-(benzyloxy)-6-bromo-*N*-(2,4-difluorobenzyl)-4-((2,4-dimethoxybenzyl)amino)-2-oxo-1,2-dihydro-1,8-naphthyridine-3-carboxamide **17c**[31] with commercial available *N*-isopropylacrylamide as outlined in general procedure K provided **18f** as a colorless oil (93% yield). ^{1}H NMR (400 MHz, CDCl$_3$) δ 12.14 (t, J = 6.8 Hz, 1H),

10.75 (t, J = 5.7 Hz, 1H), 8.65 (d, J = 1.8 Hz, 1H), 8.35 (d, J = 1.8 Hz, 1H), 7.69-7.64 (m, 2H),

7.51-7.51 (m, 1H), 7.48-7.42 (m, 3H), 7.40-7.33 (m, 3H), 6.87-6.79 (m, 2H), 6.58 (dd, J = 8.3,

2.2 Hz, 1H), 6.54 (d, J = 2.2 Hz, 1H), 5.44 (d, J = 15.6 Hz, 1H), 5.25 (s, 2H), 4.71 (d, J = 6.8 Hz,

2H), 4.61 (t, J = 9.6 Hz, 2H), 4.24-4.16 (m, 1H), 3.86 (s, 3H), 3.79 (s, 3H), 1.24 (s, 3H), 1.23 (s,

3H). ESI-MS *m/z*: 698.2 (MH[+]), 720.2 (MNa[+]).

(*E*)-1-(benzyloxy)-*N*-(2,4-difluorobenzyl)-4-((2,4-dimethoxybenzyl)amino)-6-(3-((2-hydroxyethyl)amino)-3-oxoprop-1-en-1-yl)-2-oxo-1,2-dihydro-1,8-naphthyridine-3-carboxamide (18g). Treatment of 1-(benzyloxy)-6-bromo-*N*-(2,4-difluorobenzyl)-4-((2,4-dimethoxybenzyl)amino)-2-oxo-1,2-dihydro-1,8-naphthyridine-3-carboxamide **17c**[31] with commercial available *N*-(2-hydroxyethyl)acrylamide as outlined in general procedure K provided **18g** (84% yield). ^{1}H NMR (400 MHz, CDCl$_3$) δ 6.54 (s, 1H),

6.31 (d, J = 17.0 Hz, 1H), 6.16 (dd, J = 17.0, 10.2 Hz, 1H), 5.69 (d, J = 10.2 Hz, 1H), 3.77 (t, J = 5.0 Hz, 2H), 3.51 (dd, J = 9.8, 4.9 Hz, 2H), 3.31 (d, J = 25.1 Hz, 1H).

42

(*E*)-Methyl 3-(8-(Benzyloxy)-6-((2,4-difluorobenzyl)carbamoyl)-5-((2,4-dimethoxybenzyl)amino)-7-oxo-7,8-dihydro-1,8-naphthyridin-3-yl)acrylate (18h).
Treatment of 1-(benzyloxy)-6-bromo-*N*-(2,4-difluorobenzyl)-4-((2,4-dimethoxybenzyl)amino)-2-oxo-1,2-dihydro-1,8-naphthyridine-3-carboxamide **17c**[31] with commercial available methyl acrylate as outlined in general procedure K provided **18h** as a colorless oil (38% yield). ^{1}H NMR (500 MHz, CDCl$_3$) δ 12.35 (t, *J* = 6.6 Hz, 1H), 10.73 (t, *J* = 5.6 Hz, 1H), 8.72 (s, 1H), 8.40 (s, 1H), 7.69 – 7.66 (m, 2H), 7.59 (d, *J* = 16.1 Hz, 1H), 7.42-7.38 (m, 4H), 7.23 (d, *J* = 8.0 Hz, 1H), 6.88 – 6.82 (m, 2H), 6.57 (d, *J* = 1.9 Hz, 1H), 6.54 – 6.50 (m, 1H), 6.34-6.32 (d, *J* = 8.3 Hz, 1H), 6.02 (d, *J* = 16.0 Hz, 1H), 5.27 (s, 2H), 4.78 (d, *J* = 6.7 Hz, 2H), 4.64 (d, *J* = 5.7 Hz, 2H), 3.85 (s, 3H), 3.85 (s, 3H), 3.83 (s, 3H).

Methyl 2-((1-(Benzyloxy)-3-((2,4-difluorobenzyl)carbamoyl)-6-(5-hydroxypent-1-yn-1-yl)-2-oxo-1,2-dihydro-1,8-naphthyridin-4-yl)amino)acetate (18i). Treatment of **17d** with commercial available pent-4-yn-1-ol as outlined in general procedure J provided **18i** as a colorless oil (45% yield). ^{1}H NMR (500 MHz, CDCl$_3$) δ 12.33 (s, 1H), 10.65 (t, *J* = 5.7 Hz, 1H), 8.69 (s, 1H), 8.19 (s, 1H), 7.67 – 7.65 (m, 2H), 7.43-7.37 (m, 4H), 6.87 – 6.80 (m, 2H), 5.24 (s, 2H), 4.67 (d, *J* = 5.6 Hz, 2H), 4.46 (d, *J* = 4.9 Hz, 2H), 3.84 (s, 3H), 3.85 – 3.83 (m, 2H), 2.61 (t, *J* = 7.0 Hz, 2H), 1.91 (t, *J* = 6.5 Hz, 2H). ESI-MS *m/z*: 591.2 (MH[+]).

1-(Benzyloxy)-*N*-(2,4-difluorobenzyl)-4-((2-hydroxyethyl)amino)-6-(5-hydroxypent-1-yn-1-yl)-2-oxo-1,2-dihydro-1,8-naphthyridine-3-carboxamide (18j). Treatment of **17e** with commercial available pent-4-yn-1-ol as outlined in general procedure J provided **18j** as a colorless oil (57% yield). ^{1}H NMR (500 MHz, CDCl$_3$) δ 11.68

43

(s, 1H), 10.69 (t, *J* = 5.5 Hz, 1H), 8.61 (d, *J* = 1.8 Hz, 1H), 8.32 (d, *J* = 1.8 Hz, 1H), 7.61-7.57 (m, 2H), 7.32 – 7.29 (m, 4H), 6.79 – 6.72 (m, 2H), 5.16 (s, 2H), 4.55 (d, *J* = 5.5 Hz, 2H), 3.86 – 3.84 (m, 2H), 3.80 – 3.75 (m, 2H), 2.52 (t, *J* = 7.0 Hz, 2H), 1.84 – 1.82 (m, 2H), 1.53 – 1.49 (m, 2H). ESI-MS *m/z*: 563.2 (MH+).

(*E*)-Methyl 3-(8-(Benzyloxy)-6-((2,4-difluorobenzyl)carbamoyl)-5-((2-hydroxyethyl)amino)-7-oxo-7,8-dihydro-1,8-naphthyridin-3-yl)acrylate (18k).

Treatment of **17e** with commercial available methyl acrylate as outlined in general procedure K provided **18k** as a colorless oil (52% yield). ^{1}H NMR (500 MHz, CDCl$_3$) *δ* 11.82 (s, 1H), 10.71 (s, 1H), 8.84 (s, 1H), 8.67 (s, 1H), 7.74 (d, *J* = 16.2 Hz, 1H), 7.58-7.55 (m, 2H), 7.41-7.38 (m, 4H), 6.87 – 6.81 (m, 2H), 6.55 (d, *J* = 16.1 Hz, 1H), 5.26 (s, 2H), 4.64 (d, *J* = 5.6 Hz, 2H), 3.85 (s, 3H), 3.60 (t, *J* = 4.9 Hz, 2H), 2.62 – 2.60 (m, 2H). ESI-MS *m/z*: 565.2 (MH+).

3-(5-Amino-8-(benzyloxy)-6-((2,4-difluorobenzyl)carbamoyl)-7-oxo-7,8-dihydro-1,8-naphthyridin-3-yl)prop-2-yn-1-yl Acetate (19a). Compound 4-amino-1-(benzyloxy)-*N*-(2,4-difluorobenzyl)-6-(3-hydroxyprop-1-yn-1-yl)-2-oxo-1,2-dihydro-1,8-naphthyridine-3-carboxamide[31] (29 mg, 0.06 mmol) was mixed with acetic anhydride (8.4 μl, 0.09 mmol) in pyridine (0.5 mL). The solution was stirred at room temperature (2 h). The crude mixture was purified by silica gel chromatography to provide **19a** as a colorless oil (24 mg, 76% yield). ^{1}H NMR (500 MHz, CDCl$_3$) *δ* 10.54 (t, *J* = 5.7 Hz, 1H), 8.77 (d, *J* = 1.7 Hz, 1H), 8.16 (d, *J* = 1.7 Hz, 1H), 7.65 (dd, *J* = 7.5, 1.6 Hz, 2H), 7.42 – 7.33 (m, 4H), 6.87 – 6.80 (m, 2H), 5.25 (s, 2H), 4.93 (s, 2H), 4.63 (d, *J* = 5.7 Hz, 2H), 2.16 (s, 3H). ESI-MS *m/z*: 533.2 (MH+).

4-Amino-1-(benzyloxy)-6-(3-cyclohexylprop-1-yn-1-yl)-*N*-(2,4-difluorobenzyl)-2-oxo-1,2-dihydro-1,8-naphthyridine-3-carboxamide (19b).

Treatment of **18a** as outlined in general procedure H provided **19b** as a colorless oil (91% yield). ^{1}H NMR (500 MHz, CDCl$_3$) δ 10.60 (t, *J* = 5.8 Hz, 1H), 8.74 (d, *J* = 1.8 Hz, 1H), 8.03 (d, *J* = 1.9 Hz, 1H), 7.66 (dd, *J* = 7.5, 1.8 Hz, 2H), 7.42 – 7.35 (m, 4H), 6.87 – 6.80 (m, 2H), 5.25 (s, 2H), 4.63 (d, *J* = 5.8 Hz, 2H), 2.34 (d, *J* = 6.7 Hz, 2H), 1.88 (dd, *J* = 13.5, 1.9 Hz, 2H), 1.78 – 1.74 (m, 2H), 1.70 (ddd, *J* = 12.6, 5.0, 2.6 Hz, 1H), 1.62 – 1.55 (m, 1H), 1.34 – 1.25 (m, 2H), 1.22 – 1.16 (m, 1H), 1.07 (ddd, *J* = 24.4, 12.4, 3.3 Hz, 2H). ESI-MS *m/z*: 557.2 (MH$^+$).

4-Amino-1-(benzyloxy)-*N*-(2,4-difluorobenzyl)-2-oxo-6-(4-phenylbut-1-yn-1-yl)-1,2-dihydro-1,8-naphthyridine-3-carboxamide (19c). Treatment of **18b** as outlined in general procedure H provided **19c** as a colorless oil (94% yield). ^{1}H NMR (500 MHz, CDCl$_3$) δ 10.61 (t, *J* = 5.8 Hz, 1H), 8.69 (s, 1H), 8.00 (s, 1H), 7.65 (dd, *J* = 7.1, 1.7 Hz, 2H), 7.39-7.32 (m, 6H), 7.28-7.26 (m, 3H), 6.87 – 6.80 (m, 2H), 5.24 (s, 2H), 4.63 (d, *J* = 5.8 Hz, 2H), 2.94 (t, *J* = 7.4 Hz, 2H), 2.74 (t, *J* = 7.5 Hz, 2H). ESI-MS *m/z*: 565.2 (MH$^+$).

(*E*)-4-Amino-1-(benzyloxy)-*N*-(2,4-difluorobenzyl)-2-oxo-6-styryl-1,2-dihydro-1,8-naphthyridine-3-carboxamide (19d). Treatment of **18c** as outlined in general procedure H provided **19d** as a colorless oil (68% yield). ^{1}H NMR (500 MHz, CDCl$_3$) δ 10.65 (t, *J* = 5.4 Hz, 1H), 8.89 (s, 1H), 8.12 (s, 1H), 7.81 (d, *J* = 8.3 Hz, 1H), 7.68 (d, *J* = 7.1 Hz, 2H), 7.63 (d, *J* = 7.0 Hz, 1H), 7.53 (d, *J* = 8.1 Hz, 2H), 7.40-7.38 (m,4H), 7.33 – 7.30 (m, 1H), 7.17 (dd, *J* = 47.6, 17.5 Hz, 2H), 6.89 – 6.79 (m, 2H), 5.28 (s, 2H), 4.64 (d, *J* = 5.2 Hz, 2H). ESI-MS *m/z*: 539.2 (MH$^+$).

45

4-Amino-1-(benzyloxy)-*N*-(2,4-difluorobenzyl)-6-(3-(dimethylamino)prop-1-yn-1-yl)-2-oxo-1,2-dihydro-1,8-naphthyridine-3-carboxamide (19e). Treatment of 1-(benzyloxy)-6-bromo-*N*-(2,4-difluorobenzyl)-4-((2,4-dimethoxybenzyl)amino)-2-oxo-1,2-dihydro-1,8-naphthyridine-3-carboxamide **17c**[31] with commercial available *N,N*-dimethylprop-2-yn-1-amine as outlined in general procedures J and H provided **19e** as a colorless oil (33% yield, two steps). ^{1}H NMR (500 MHz, CDCl₃) δ 10.57 (t, *J* = 5.7 Hz, 1H), 8.77 (d, *J* = 1.6 Hz, 1H), 8.11 (d, *J* = 1.6 Hz, 1H), 7.67 – 7.65 (m, 2H), 7.42 – 7.36 (m, 4H), 6.87 – 6.80 (m, 2H), 5.25 (s, 2H), 4.63 (d, *J* = 5.7 Hz, 2H), 3.51 (s, 2H), 2.42 (s, 6H). ESI-MS *m/z*: 518.2 (MH⁺).

4-Amino-1-(benzyloxy)-*N*-(2,4-difluorobenzyl)-6-(3-(2-hydroxyethoxy)prop-1-yn-1-yl)-2-oxo-1,2-dihydro-1,8-naphthyridine-3-carboxamide (19f). Treatment of **18d** as outlined in general procedure H provided **19f** as a colorless oil (87% yield). ^{1}H NMR (500 MHz, CDCl₃) δ 10.55 (t, *J* = 5.7 Hz, 1H), 8.79 (d, *J* = 1.7 Hz, 1H), 8.08 (d, *J* = 1.8 Hz, 1H), 7.68 – 7.67 (m, 2H), 7.41 – 7.38 (m, 4H), 6.88 – 6.82 (m, 2H), 5.27 (s, 2H), 4.64 (d, *J* = 5.8 Hz, 2H), 4.49 (s, 2H), 3.86 – 3.84 (m, 2H), 3.77 – 3.75 (m, 2H). ESI-MS *m/z*: 535.2 (MH⁺).

(*E*)-Methyl 3-(5-Amino-8-(benzyloxy)-6-((2,4-difluorobenzyl)carbamoyl)-7-oxo-7,8-dihydro-1,8-naphthyridin-3-yl)acrylate (19g). Treatment of **18h** as outlined in general procedure H provided **19g** as a colorless oil (38% yield). ^{1}H NMR (500 MHz, CDCl₃) δ 10.54 (d, *J* = 5.6 Hz, 1H), 8.89 (d, *J* = 1.5 Hz, 1H), 8.13 (s, 1H), 7.76 (d, *J* = 16.1 Hz, 1H), 7.67 (d, *J* = 6.1 Hz, 2H), 7.41-7.37 (m, 4H), 6.87 – 6.81 (m, 2H), 6.59 (d, *J* = 16.1 Hz, 1H), 5.27 (s, 2H), 4.64 (d, *J* = 5.7 Hz, 2H), 3.86 (s, 3H). ESI-MS *m/z*: 521.2 (MH⁺).

HIV-1 IN Biochemical Assays. As previously described,[43] inhibitors or an equivalent volume of DMSO were added to a reaction mixture containing 20 nM DNA substrate 5' ^{32}P-labeled on the transferred strand and 400 nM IN in 50 mM MOPS pH 7.2, 7.5 mM MgCl$_2$, and 14 mM 2-mercaptoethanol. Reactions were allowed to proceed for 2 h at 37 °C and were stopped by the addition of an equal volume of loading buffer [1% sodium dodecyl sulfate, 0.025% bromophenol blue, and 0.025% xylene cyanol made in formamide]. Reaction products, separated in 16% polyacrylamide denaturing sequencing gels, were visualized using by phosphorimaging using a Typhoon 8600 instrument (GE Healthcare) and quantified using the ImageQuant 5.1 software (GE Healthcare). Data analyses (linear regression, IC$_{50}$ determination, and standard deviation) were performed using Prism 5.0 software from GraphPad.

HIV-1 Vector Constructs. pNLNgoMIVR$^-$ΔEnv.LUC has been described previously.[44] The IN reading frame was removed from pNLNgoMIVR$^-$ΔEnv.LUC by digestion with KpnI and SalI and inserted between the KpnI and SalI sites of pBluescript II KS+. With this construct as the WT template, the following HIV-1 IN mutants were prepared using the QuikChange II XL (Stratagene, La Jolla, CA) site-directed mutagenesis protocol: H51Y, T66I, E92Q, G118R, Y143R, Q148H, N155H, R263K, G140S + Q148H, and H51Y + R263K. The following sense and cognate antisense (not shown) oligonucleotides (Integrated DNA Technologies, Coralville, IA) were used in the mutagenesis: H51Y, 5'-CTAAAAGGGGAAGCCATGTATGGACAAGTAGACTGTA-3'; T66I, 5'-CCAGGAATATGGCAGCTAGATTGTATACATTTAGAAGGAAAAGTT-3'; E92Q, 5'-GCAGAAGTAATTCCAGCACAGACAGGGCAAGAAA -3'; G118R, 5'-

47

GTACATACAGACAATCGCAGCAATTTCACCAGTAC-3'; G140S, 5'-

GGGGATCAAGCAGGAATTTAGCATTCCCTACAATC-3'; Y143C, 5'-

GCAGGAATTTGGCATTCCCCGCAATCCCCAAAGTCAAGGA-3'; Q148H, 5'-

CATTCCCTACAATCCCCAAAGTCATGGAGTAATAGAATCTA -3'; N155H, 5'-

CCAAAGTCAAGGAGTAATAGAATCTATGCATAAAGAATTAAAGAAAATTATAGGACA-3';

R263K 5'- AAAGTAGTGCCAAGAAAAAAAGCAAAGATCATC -3'. The double mutation G140S +

Q148H was constructed using the previously generated Q148H mutant and the appropriate

oligonucleotides to introduce the second mutation, G140S. The double mutation H51Y +

R263K was constructed by using the previously generated H51Y mutant and the

appropriate oligonucleotides for the second mutation, R263K. The DNA sequence of each

construct was verified by DNA sequencing. The mutant IN coding sequences from

pBluescript II KS+ were subcloned into pNLNgoMIVR⁻ΔEnv.LUC (between the KpnI and SalI

sites) to produce the full-length mutant HIV-1 IN constructs. The mutant forms of the

vector were validated by DNA sequence determination.

Single-round HIV-1 Infectivity Assay. Assays were performed using the human

embryonic kidney cell culture cell line 293 acquired from the American Type Culture

Collection (ATCC) and the human osteosarcoma cell line, HOS, obtained from Dr. Richard

Schwartz (Michigan State University, East Lansing, MI) using methods that have been

previously reported.[44, 45] The 293 and HOS cells were grown in Dulbecco's modified Eagle's

medium (Invitrogen, Carlsbad, CA) supplemented with 5% (v/v) fetal bovine serum, 5%

newborn calf serum, and penicillin (50 units/mL) plus streptomycin (50 μg/mL; Quality

Biological, Gaithersburg, MD). The transfection vector, pNLNgoMIVR⁻ΔLUC was made from

48

pNLNgoMIVR-ΔEnv.HSA by removing the HSA reporter gene and replacing it with a luciferase reporter gene, which was inserted between the NotI and XhoI restriction sites.[44] VSV-g-pseudotyped HIV was produced by transfection of 293 cells.[45] On the day prior to transfection, 293 cells were plated on 100-mm-diameter dishes at a density of 1.5×10^6 cells per plate and transfected with 16 µg of pNLNgoMIVR-ΔLUC and 4 µg of pHCMV-g (obtained from Dr. Jane Burns, University of California, San Diego) using the calcium phosphate method. At approximately 6 h after the calcium phosphate precipitate was added, 293 cells were washed twice with phosphate-buffered saline (PBS) and incubated with fresh media for 48 h. The virus-containing supernatants were harvested, clarified by low-speed centrifugation, filtered, and diluted for use in antiviral infection assays. On the day prior to the screen, HOS cells were seeded in 96-well luminescence cell culture plates at a density of 4000 cells in 100 µL per well. On the day of the assay for cellular cytotoxicity, cells were treated with compounds using a concentration range from 250 µM to 0.05 µM and then incubated at 37 °C (48 h). On the day of the assay for antiviral activity, cells were treated with compounds using a concentration range from 5 µM to 0.0001 µM using 11 serial dilutions and then incubated at 37 °C (3 h). After 3h, 100 µL of virus-stock [diluted to achieve a luciferase signal between 0.2 and 1.5 Relative Luciferase Units (RLUs)] was added to each well and incubation was continued (37 °C, 48 h). Cellular cytotoxicity was measured by using the ATP Lite Luminescence detection system and monitored by adding 50 µL of cell lysis buffer from the Luminescence ATP detection assay to each well followed by mixing at 700 rpm at room temperature using a compact thermomixer (5 minutes). After addition of 50 µL of reconstituted Luminescence ATP detection assay reagent to all wells except for the negative control/background wells, the plates were mixed at 700 rpm at

49

room temperature using a compact thermomixer (5 minutes), incubated at room

temperature to allow time for signal development (20 minutes), and cytotoxicity was

determined using the microplate reader. Infectivity was measured using the Steady-lite

plus luminescence reporter gene assay system (PerkinElmer, Waltham, MA). Luciferase

activity was measured by adding 100 µL of Steady-lite plus buffer (PerkinElmer) to the

cells, incubating at room temperature (20 minutes), and measuring luminescence using a

microplate reader. Both cytotoxicity and antiviral activity were normalized to the cellular

cytotoxicity and infectivity using cells incubated in absence of the respective target

compounds. KaleidaGraph (Synergy Software, Reading, PA) was used to perform non-linear

regression analysis on the data. Final IC_{50} values were determined from the fit model.

X-Ray Crystallography. PFV intasome crystals were soaked in the presence of 0.5-1 mM

INSTIs in cryoprotection solution prior to snap freezing in liquid nitrogen as described.[23, 24]

X-ray diffraction data collected on beamlines I04 and I03 of the Diamond Light Source

(Oxfordshire, UK) was processed using XDS[46] and Aimless.[47] Structures were determined

via rigid-body refinement of model generated from PDB ID 4BDZ by removing small

molecule atoms, and the compounds were fitted into resulting *Fo-Fc* difference maps. The

models were built in Coot,[48] refined in Phenix,[49] and validated using MolProbity.[50] Relevant

data collection and refinement statistics are given in Table 5.

ASSOCIATED CONTENT

Supporting Information

50

Supporting Information. Figure S1 presenting overlays of the PFV crystal structures of

several bound INSTIs highlighting the correspondence of features corresponding to the 4-

position of the current compounds, Table S1 containing predicted molPAINS values for

final products and molecular formula strings.

Accession Codes

Atomic coordinates and structure factors for PFV intasome-bound **5′g**, **5g** and **6p** have

been deposited in the RCSB Protein Data Bank (PDB codes 5MMA, 5NO1 and 5MMB

respectively). Authors will release the atomic coordinates and experimental data upon

article publication.

AUTHOR INFORMATION

Corresponding Author

*E-mail: burkete@helix.nih.gov. Telephone: 301-846-5906.

Notes

The authors declare the following competing financial interest: Compounds contained in

the current publication are contained within filed patent applications.

ABBREVIATIONS USED

51

HIV-1, human immunodeficiency virus type 1; PFV, prototype foamy virus; AIDS, acquired

immune deficiency syndrome; FDA, Food and Drug Administration; IN, integrase; RAL,

raltegravir; EVG, elvitegravir; DTG, dolutegravir; 3-P, 3-processing; ST, strand transfer;

INSTIs, integrase strand transfer inhibitors; DNA, deoxyribonucleic acid; IC_{50}, half-

maximum inhibitory concentration; EC_{50}, half maximal effective concentration; WT, wild-

type; DMF, dimethylformamide; HPLC, high-pressure liquid chromatography; HRMS, high-

resolution mass spectrometry; PBS, phosphate-buffered saline; RLUs, relative luciferase

units.

REFERENCES

1.   Lesbats, P.; Engelman, A. N.; Cherepanov, P. Retroviral DNA integration. *Chem. Rev.*
2016, *116*, 12730-12757.

2.   Summa, V.; Petrocchi, A.; Bonelli, F.; Crescenzi, B.; Donghi, M.; Ferrara, M.; Fiore, F.;
Gardelli, C.; Gonzalez Paz, O.; Hazuda, D. J.; Jones, P.; Kinzel, O.; Laufer, R.; Monteagudo, E.;
Muraglia, E.; Nizi, E.; Orvieto, F.; Pace, P.; Pescatore, G.; Scarpelli, R.; Stillmock, K.; Witmer, M.
V.; Rowley, M. Discovery of raltegravir, a potent, selective orally bioavailable HIV-integrase
inhibitor for the treatment of HIV-AIDS infection. *J. Med. Chem.* **2008,** *51*, 5843-5855.

3.   Sato, M.; Motomura, T.; Aramaki, H.; Matsuda, T.; Yamashita, M.; Ito, Y.; Kawakami, H.;
Matsuzaki, Y.; Watanabe, W.; Yamataka, K.; Ikeda, S.; Kodama, E.; Matsuoka, M.; Shinkai, H.
Novel HIV-1 integrase inhibitors derived from quinolone antibiotics. *J. Med. Chem.* **2006,** *49*,
1506-1508.

4.   Johns, B. A.; Kawasuji, T.; Weatherhead, J. G.; Taishi, T.; Temelkoff, D. P.; Yoshida, H.;
Akiyama, T.; Taoda, Y.; Murai, H.; Kiyama, R.; Fuji, M.; Tanimoto, N.; Jeffrey, J.; Foster, S. A.;

Yoshinaga, T.; Seki, T.; Kobayashi, M.; Sato, A.; Johnson, M. N.; Garvey, E. P.; Fujiwara, T. Carbamoyl pyridone HIV-1 integrase Inhibitors 3. A diastereomeric approach to chiral nonracemic tricyclic ring systems and the discovery of dolutegravir (S/GSKi349572) and (S/GSK1265744). *J. Med. Chem.* **2013,** *56*, 5901-5916.

5.   Hazuda, D. J.; Felock, P.; Witmer, M.; Wolfe, A.; Stillmock, K.; Grobler, J. A.; Espeseth, A.; Gabryelski, L.; Schleif, W.; Blau, C.; Miller, M. D. Inhibitors of strand transfer that prevent integration and inhibit HIV-1 replication in cells. *Science* **2000,** *287*, 646 - 650.

6.   Métifiot, M.; Johnson, B. C.; Kiselev, E.; Marler, L.; Zhao, X. Z.; Burke, T. R.; Marchand, C.; Hughes, S. H.; Pommier, Y. Selectivity for strand-transfer over 3′-processing and susceptibility to clinical resistance of HIV-1 integrase inhibitors are driven by key enzyme–DNA interactions in the active site. *Nucleic Acids Res.* **2016,** *44*, 6896-6906.

7.   Bar-Magen, T.; Sloan, R. D.; Faltenbacher, V. H.; Donahue, D. A.; Kuhl, B. D.; Oliveira, M.; Xu, H.; Wainberg, M. A. Comparative biochemical analysis of HIV-1 subtype B and C integrase enzymes. *Retrovirology* **2009,** *6*, 103.

8.   Hare, S.; Maertens, G. N.; Cherepanov, P. 3'-Processing and strand transfer catalysed by retroviral integrase in crystallo. *EMBO J.* **2012,** *31*, 3020-3028.

9.   Abram, M. E.; Ferris, A. L.; Shao, W.; Alvord, W. G.; Hughes, S. H. Nature, position, and frequency of mutations made in a single cycle of HIV-1 replication. *J. Virol.* **2010,** *84*, 9864-9878.

10.   Wainberg, M. A.; Zaharatos, G. J.; Brenner, B. G. Development of antiretroviral drug resistance. *N. Engl. J. Med.* **2011,** *365*, 637-646.

11.   Garrido, C.; Villacian, J.; Zahonero, N.; Pattery, T.; Garcia, F.; Gutierrez, F.; Caballero, E.; Van, H. M.; Soriano, V.; de, M. C. Broad phenotypic cross-resistance to elvitegravir in HIV-

53

infected patients failing on raltegravir-containing regimens. *Antimicrob. Agents Chemother.* **2012,** *56*, 2873-2878.

12.   Geretti, A. M.; Armenia, D.; Ceccherini-Silberstein, F. Emerging patterns and implications of HIV-1 integrase inhibitor resistance. *Curr. Opin. Infect. Dis.* **2012,** *25*, 677-686.

13.   Quashie, P. K.; Mesplede, T.; Wainberg, M. A. Evolution of HIV integrase resistance mutations. *Curr. Opin. Infect. Dis.* **2013,** *26*, 43-49.

14.   Ballantyne, A. D.; Perry, C. M. Dolutegravir: First global approval. *Drugs* **2013,** *73*, 1627-1637.

15.   Hurt, C. B.; Sebastian, J.; Hicks, C. B.; Eron, J. J. Resistance to HIV integrase strand transfer inhibitors among clinical specimens in the united states, 2009-2012. *Clin. Infect. Dis.* **2014,** *58*, 423-431.

16.   McCormack, P. L. Dolutegravir: A review of its use in the management of HIV-1 infection in adolescents and adults. *Drugs* **2014,** *74*, 1241-1254.

17.   Mesplede, T.; Quashie, P. K.; Wainberg, M. A. Resistance to HIV integrase inhibitors. *Curr. Opin. HIV AIDS* **2012,** *7*, 401-408.

18.   Li, M.; Mizuuchi, M.; Burke, T. R., Jr.; Craigie, R. Retroviral DNA integration: reaction pathway and critical intermediates. *EMBO J.* **2006,** *25*, 1295-1304.

19.   Hare, S.; Gupta, S.; Valkov, E.; Engelman, A.; Cherepanov, P. Retroviral intasome assembly and inhibition of DNA strand transfer. *Nature* **2010,** *464*, 232 - 236.

20.   Passos, D. O.; Li, M.; Yang, R.; Rebensburg, S. V.; Ghirlando, R.; Jeon, Y.; Shkriabai, N.; Kvaratskhelia, M.; Craigie, R.; Lyumkis, D. Cryo-EM structures and atomic model of the HIV-1 strand transfer complex intasome. *Science* **2017,** *355*, 89-92.

54

21.   Ballandras-Colas, A.; Maskell, D. P.; Serrao, E.; Locke, J.; Swuec, P.; Jónsson, S. R.; Kotecha, A.; Cook, N. J.; Pye, V. E.; Taylor, I. A.; Andrésdóttir, V.; Engelman, A. N.; Costa, A.; Cherepanov, P. A supramolecular assembly mediates lentiviral DNA integration. *Science* **2017,** *355*, 93-95.

22.   Espeseth, A. S.; Felock, P.; Wolfe, A.; Witmer, M.; Grobler, J.; Anthony, N.; Egbertson, M.; Melamed, J. Y.; Young, S.; Hamill, T.; Cole, J. L.; Hazuda, D. J. HIV-1 integrase inhibitors that compete with the target DNA substrate define a unique strand transfer conformation for integrase. *Proc. Natl. Acad. Sci. U.S.A.* **2000,** *97*, 11244-11249.

23.   Hare, S.; Smith, S. J.; Metifiot, M.; Jaxa-Chamiec, A.; Pommier, Y.; Hughes, S. H.; Cherepanov, P. Structural and functional analyses of the second-generation integrase strand transfer inhibitor dolutegravir (S/GSK1349572). *Mol. Pharmacol.* **2011,** *80*, 565-572.

24.   Hare, S.; Vos, A. M.; Clayton, R. F.; Thuring, J. W.; Cummings, M. D.; Cherepanov, P. Molecular mechanisms of retroviral integrase inhibition and the evolution of viral resistance. *Proc. Natl. Sci. U. S. A.* **2010,** *107*, 20057-20062.

25.   Pommier, Y.; Marchand, C. Interfacial inhibitors: targeting macromolecular complexes. *Nat. Rev. Drug Discovery* **2012,** *11*, 25-36.

26.   Zhao, X. Z.; Smith, S. J.; Metifiot, M.; Johnson, B. C.; Marchand, C.; Pommier, Y.; Hughes, S. H.; Burke, T. R., Jr. Bicyclic 1-hydroxy-2-oxo-1,2-dihydropyridine-3-carboxamide-containing HIV-1 integrase inhibitors having high antiviral potency against cells harboring raltegravir-resistant integrase mutants. *J. Med. Chem.* **2014,** *57*, 1573-1582.

27.   Zhao, X. Z.; Smith, S. J.; Metifiot, M.; Marchand, C.; Boyer, P. L.; Pommier, Y.; Hughes, S. H.; Burke, T. R., Jr. 4-Amino-1-hydroxy-2-oxo-1,8-naphthyridine-containing compounds

having high potency against raltegravir-resistant integrase mutants of HIV-1. *J. Med. Chem.* **2014,** *57*, 5190-5202.

28.   Wensing, A. M.; Calvez, V.; Günthard, H. F.; Johnso, V. A.; Pare, R.; Pill, D.; Shafer, R. W.; Richman, D. D. 2017 Update of the drug resistance mutations in HIV-1. *Top. Anitivir. Med.* **2017,** *14*, 132-141.

29.   Kawasuji, T.; Johns, B. A.; Yoshida, H.; Weatherhead, J. G.; Akiyama, T.; Taishi, T.; Taoda, Y.; Mikamiyama-Iwata, M.; Murai, H.; Kiyama, R.; Fuji, M.; Tanimoto, N.; Yoshinaga, T.; Seki, T.; Kobayashi, M.; Sato, A.; Garvey, E. P.; Fujiwara, T. Carbamoyl pyridone HIV-1 integrase inhibitors. 2. Bi- and tricyclic derivatives result in superior antiviral and pharmacokinetic profiles. *J. Med. Chem.* **2013,** *56*, 1124-1135.

30.   Raheem, I. T.; Walji, A. M.; Klein, D.; Sanders, J. M.; Powell, D. A.; Abeywickrema, P.; Barbe, G.; Bennet, A.; Clas, S. D.; Dubost, D.; Embrey, M.; Grobler, J.; Hafey, M. J.; Hartingh, T. J.; Hazuda, D. J.; Miller, M. D.; Moore, K. P.; Pajkovic, N.; Patel, S.; Rada, V.; Rearden, P.; Schreier, J. D.; Sisko, J.; Steele, T. G.; Truchon, J. F.; Wai, J.; Xu, M.; Coleman, P. J. Discovery of 2-pyridinone aminals: A prodrug strategy to advance a second generation of HIV-1 integrase strand transfer inhibitors. *J. Med. Chem.* **2015,** *58*, 8154-8165.
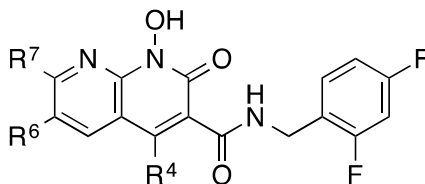
31.   Zhao, X. Z.; Smith, S.; Maskell, D.; Metifiot, M.; Pye, V.; Fesen, K.; Marchand, C.; Pommier, Y.; Cherepanov, P.; Hughes, S.; Burke, T. R. HIV-1 integrase strand transfer inhibitors with reduced susceptibility to drug resistant mutant integrases. *ACS Chem. Biol.* **2016,** *11*, 1074-1081.

32.   Wainberg, M. A.; Mesplede, T.; Raffi, F. What if HIV were unable to develop resistance against a new therapeutic agent? *BMC Med.* **2013,** *11*, 249.

33.   Shah, B. M.; Schafer, J. J.; DeSimone, J. A., Jr. Dolutegravir: A new integrase strand transfer inhibitor for the treatment of HIV. *Pharmacotherapy* **2014,** *34*, 506-520.

34.   Malet, I.; Gimferrer Arriaga, L.; Artese, A.; Costa, G.; Parrotta, L.; Alcaro, S.; Delelis, O.; Tmeizeh, A.; Katlama, C.; Valantin, M.-A.; Ceccherini-Silberstein, F.; Calvez, V.; Marcelin, A.-G. New raltegravir resistance pathways induce broad cross-resistance to all currently used integrase inhibitors. *J. Antimicrob. Chemother.* **2014,** *69*, 2118-2122.

35.   King, N. M.; Prabu-Jeyabalan, M.; Nalivaika, E. A.; Schiffer, C. A. Combating susceptibility to drug resistance: Lessons from HIV-1 protease. *Chem. Biol.* **2004,** *11*, 1333-1338.

36.   Hirokawa, Y.; Fujiwara, I.; Suzuki, K.; Harada, H.; Yoshikawa, T.; Yoshida, N.; Kato, S. Synthesis and structure–affinity relationships of novel N-(1-ethyl-4-methylhexahydro-1,4-diazepin-6-yl)pyridine-3-carboxamides with potent serotonin 5-HT3 and dopamine D2 receptor antagonistic activity. *J. Med. Chem.* **2003,** *46*, 702-715.

37.   LaFemina, R. L.; Graham, P. L.; LeGrow, K.; Hastings, J. C.; Wolfe, A.; Young, S. D.; Emini, E. A.; Hazuda, D. J. Inhibition of human immunodeficiency virus integrase by bis-catechols. *Antimicrob. Agents Chemother.* **1995,** *39*, 320-324.

38.   Charpentier, C.; Karmochkine, M.; Laureillard, D.; Tisserand, P.; Belec, L.; Weiss, L.; Si-Mohamed, A.; Piketty, C. Drug resistance profiles for the HIV integrase gene in patients failing raltegravir salvage therapy. *HIV Med.* **2008,** *9*, 765-70.

39.   Cooper, D. A.; Steigbigel, R. T.; Gatell, J. M.; Rockstroh, J. K.; Katlama, C.; Yeni, P.; Lazzarin, A.; Clotet, B.; Kumar, P. N.; Eron, J. E.; Schechter, M.; Markowitz, M.; Loutfy, M. R.; Lennox, J. L.; Zhao, J.; Chen, J.; Ryan, D. M.; Rhodes, R. R.; Killar, J. A.; Gilde, L. R.; Strohmaier, K. M.; Meibohm, A. R.; Miller, M. D.; Hazuda, D. J.; Nessly, M. L.; DiNubile, M. J.; Isaacs, R. D.;

57

Teppler, H.; Nguyen, B.-Y. Subgroup and resistance analyses of raltegravir for resistant HIV-1 infection. *N. Engl. J. Med.* **2008,** *359*, 355-365.

40. Shen, Y.; Altman, M. D.; Ali, A.; Nalam, M. N. L.; Cao, H.; Rana, T. M.; Schiffer, C. A.; Tidor, B. Testing the substrate-envelope hypothesis with designed pairs of compounds. *ACS Chem. Biol.* **2013,** *8*, 2433-2441.

41. Das, K.; Bauman, J. D.; Clark, A. D.; Frenkel, Y. V.; Lewi, P. J.; Shatkin, A. J.; Hughes, S. H.; Arnold, E. High-resolution structures of HIV-1 reverse transcriptase/TMC278 complexes: Strategic flexibility explains potency against resistance mutations. *Proc. Natl. Acad. Sci. U. S. A.* **2008,** *105*, 1466-1471.

42. Hirokawa, Y.; Horikawa, T.; Kato, S. An efficient synthesis of 5-bromo-2-methoxy-6methylaminopyridine-3-carboxylic acid. *Chem. Pharm. Bull.* **2000,** *48*, 1847-1853.

43. Metifiot, M.; Maddali, K.; Johnson, B. C.; Hare, S.; Smith, S. J.; Zhao, X. Z.; Marchand, C.; Burke, T. R., Jr.; Hughes, S. H.; Cherepanov, P.; Pommier, Y. Activities, crystal structures and molecular dynamics of dihydro-1H-isoindole derivatives, inhibitors of HIV-1 integrase. *ACS Chem. Biol.* **2013,** *8*, 209-217.

44. Zhao, X. Z.; Maddali, K.; Metifiot, M.; Smith, S. J.; Vu, B. C.; Marchand, C.; Hughes, S. H.; Pommier, Y.; Burke, T. R., Jr. Bicyclic hydroxy-1H-pyrrolopyridine-trione containing HIV-1 integrase inhibitors. *Chem. Biol. Drug Des.* **2012,** *79*, 157-165.

45. Brachmann, A.; Koenig, J.; Julius, C.; Feldbruegge, M. A reverse genetic approach for generating gene replacement mutants in Ustilago maydis. *Mol. Genet. Genomics* **2004,** *272*, 216-226.

46. Kabsch, W. XDS. *Acta Crystallogr., Sect. D: Biol. Crystallogr.* **2010,** *66*, 125 - 132.

47.　　Evans, P. R.; Murshudov, G. N. How good are my data and what is the resolution?

Acta Crystallogr., Sect. D: Biol. Crystallogr. **2013,** *69*, 1204-1214.

48.　　Emsley, P.; Cowtan, K. Coot: Model-building tools for molecular graphics. *Acta*

Crystallogr., Sect. D: Biol. Crystallogr. **2004,** *60*, 2126-2132.

49.　　Adams, P. D.; Afonine, P. V.; Bunkóczi, G.; Chen, V. B.; Echols, N.; Headd, J. J.; Hung, L.-

W.; Jain, S.; Kapral, G. J.; Grosse Kunstleve, R. W.; McCoy, A. J.; Moriarty, N. W.; Oeffner, R. D.;

Read, R. J.; Richardson, D. C.; Richardson, J. S.; Terwilliger, T. C.; Zwart, P. H. The Phenix

software for automated determination of macromolecular structures. *Methods* **2011,** *55*,

94-106.

50.　　Chen, V. B.; Arendall, W. B., III; Headd, J. J.; Keedy, D. A.; Immormino, R. M.; Kapral, G.

J.; Murray, L. W.; Richardson, J. S.; Richardson, D. C. MolProbity: all-atom structure

validation for macromolecular crystallography. *Acta Crystallogr., Sect. D: Biol. Crystallogr.*

2010, *66*, 12-21.

51.　　Zhao, X. Z.; Semenova, E. A.; Vu, B. C.; Maddali, K.; Marchand, C.; Hughes, S. H.;

Pommier, Y.; Burke, T. R. 2,3-Dihydro-6,7-dihydroxy-1H-isoindol-1-one-based HIV-1

integrase inhibitors. *J. Med. Chem.* **2008,** *51*, 251-259.

Table 1. Inhibitory potencies of compounds using an *in vitro* IN assay.[a]

No.	R^4	R^6	R^7	*In Vitro* (IC$_{50}$ µM)	
				3'-P	ST
5'a[b]	OH	H	H	1.2 ± 0.2	0.055 ± 0.008
5a	OH	H	OCH$_3$	32 ± 4	0.033 ± 0.005
5b	OH	H	piperidinyl	> 333	70 ± 16
5c	OH	H	morpholino	> 333	1.9 ± 0.2
5'd[c]	NH$_2$	H	H	2.5 ± 0.3	0.019 ± 0.002
5d	NH$_2$	H	OCH$_3$	18 ± 2	0.011 ± 0.002
5e	NH$_2$	H	piperidinyl	> 333	54 ± 18
5f	NH$_2$	H	morpholino	> 333	54 ± 10
5'g[c]	NHCH$_2$CO$_2$CH$_3$	H	H	0.71 ± 0.10	0.021 ± 0.011
5g	NHCH$_2$CO$_2$CH$_3$	H	OCH$_3$	20 ± 2	0.042 ± 0.005
5h	NHCH$_2$CO$_2$CH$_3$	H	piperidinyl	> 333	96 ± 40
5i	NHCH$_2$CO$_2$CH$_3$	H	morpholino	> 333	6.2 ± 0.8
6a	OH	(CH$_2$)$_5$OH	H	14.3 ± 1.1	0.012 ± .003
6'b[d]	NH$_2$	(CH$_2$)$_5$OH	H	8.2 ± 1.2	0.0027 ± 0.0004

60

6b	NH_2	$(CH_2)_3OAc$	H	14.3 ± 2.1	0.010 ± 0.002
6c	NH_2	$(CH_2)_6OBz$	H	143 ± 14	3.3 ± 0.6
6d	NH_2	$(CH_2)_3{}^cHex$	H	289 ± 49	3.3 ± 0.5
6e	NH_2	$(CH_2)_4Ph$	H	42 ± 4	2.0 ± 0.4
6f	NH_2	$(CH_2)_2Ph$	H	48 ± 4	0.014 ± 0.003
6g	NH_2	$(CH_2)_3N(CH_3)_2$	H	3.0 ± 0.4	0.014 ± 0.002
6h	NH_2	$(CH_2)_3O(CH_2)_2OH$	H	1.5 ± 0.4	0.0020 ± 0.0004
6i	NH_2	$(CH_2)_2CO_2H$	H	ND^e	0.004 ± 0.001
6j	NH_2	$(CH_2)_2CON(CH_3)_2$	H	ND	0.008 ± 0.001
6k	NH_2	$(CH)_2CON(CH_3)_2$	H	ND	0.005 ± 0.001
6l	NH_2	$(CH_2)_2CONH^iPr$	H	ND	0.002 ± 0.007
6m	NH_2	$(CH)_2CONH^iPr$	H	ND	0.006 ± 0.005
6n	NH_2	$(CH_2)_2CONH(CH_2)_2OH$	H	ND	0.002 ± 0.001
6o	NH_2	$(CH)_2CONH(CH_2)_2OH$	H	ND	0.007 ± 0.001
6p	NH_2	$(CH_2)_2CO_2CH_3$	H	2.9 ± 0.6	0.0031 ± 0.0005
6q	$NHCH_2CO_2CH_3$	$(CH_2)_5OH$	H	2.1 ± 0.5	0.004 ± 0.001
6r	$NH(CH_2)_2OH$	$(CH_2)_5OH$	H	4.0 ± 0.5	0.0025 ± 0.0002
6s	$NH(CH_2)_2OH$	$(CH_2)_5OAc$	H	ND	ND
6t	$NH(CH_2)_2OH$	$(CH_2)_2CO_2CH_3$	H	3.2 ± 0.3	0.0031 ± 0.0003

61

[a]Assays were performed using a gel-based protocol with Mg^{2+} cofactor as described;[51] [b]Data have been reported previously;[26] [c]Data has been reported previously;[27] [d]Data have been reported previously.[31] [e]Not determined.

Table 2. Antiviral potencies in cells infected with HIV-1 vectors that carry WT or resistant IN mutants.[a]

No.	EC$_{50}$ (nM/FC[e])				CC$_{50}$ (μM)
	WT	**Y143R**	**N155H**	**G140S/Q148H**	
RAL (1)[b]	4 ± 2	162 ± 16 (41×)	154 ± 33 (39×)	1900 ± 300 (475×)	>250
EVG (2) [b]	6.4 ± 0.8	7.9 ± 2.3 (1×)	90 ± 18 (14×)	5700 ± 1100 (891×)	>250
DTG (3) [b]	1.6 ± 0.9	4.3 ± 1.2 (3×)	3.6 ± 1.3 (2×)	5.8 ± 0.5 (4×)	>250
5'a[c]	6.2 ± 2.9	11 ± 2 (2×)	31 ± 8 (5×)	308 ± 125 (50×)	137 ± 20
5a	215 ± 31	ND[f]	ND	ND	12 ± 5
5'd[c]	1.1 ± 0.7	2.5 ± 0.6 (2×)	5.3 ± 2.3 (5×)	35 ± 9 (32×)	>250
5d	30 ± 9	62 ± 26 (2×)	400 ± 101 (13×)	3600 ± 1600 (120×)	2.2 ± 0.4
5'g	3.8 ± 1.2	4.6 ± 2.2 (1×)	19 ± 7 (5×)	36 ± 16 (9×)	>250
5g	32 ± 13	52 ± 13 (2×)	1260 ± 320 (39×)	ND	12 ± 3
6a	24 ± 4	8.3 ± 1.7 (0.3×)	32 ± 3 (1×)	29 ± 10 (1×)	> 250
6'b[d]	1.3 ± 0.2	3.0 ± 0.5 (2×)	2.4 ± 0.8 (2×)	9.4 ± 3.6 (7×)	>250
6b	1.4 ± 0.4	2.9 ± 0.9 (2×)	5.4 ± 2.5 (4×)	13 ± 8 (9×)	>250

63

6c	4.8 ± 1.6	3.5 ± 1.2 (0.7×)	5.4 ± 1.9 (1×)	21 ± 7.8 (4×)	14.4 ± 4.8
6d	53 ± 14	112 ± 14 (2×)	146 ± 37 (3×)	ND	27.4 ± 3.1
6e	11 ± 2	4.7 ± 0 (0.4×)	39 ± 10 (4×)	128 ± 44 (12×)	13 ± 2
6f	5.6 ± 1.9	5.5 ± 2.4 (1×)	21 ± 5 (4×)	140 ± 34 (25×)	18 ± 2
6g	6.1 ± 2.1	7.0 ± 2.3 (1×)	29 ± 9 (5×)	32 ± 5 (5×)	5.0 ± 1.8
6h	1.6 ± 0.2	1.2 ± 0.6 (0.8×)	4.2 ± 1.5 (3×)	35 ± 3.7 (22×)	>250
6i	1.9 ± 0.5	4.9 ± 1.5 (3×)	10 ± 3 (5×)	195 ± 25 (103×)	>250
6j	1.3 ± 0.5	6 ± 1 (5×)	6.8 ± 1.6 (5×)	16 ± 5 (12×)	>250
6k	1.6 ± 0.9	7.2 ± 0.3 (5×)	15 ± 2 (9×)	58 ± 19 (36×)	>250
6l	5 ± 1.3	8.7 ± 2.2 (2×)	11 ± 4 (2×)	13 ± 1 (3×)	>250
6m	2.1 ± 0.7	11 ± 1 (5×)	12 ± 3 (6×)	286 ± 8 (136×)	>250
6n	263 ± 52	ND	ND	ND	>250
6o	196 ± 32	ND	ND	ND	>250
6p	0.67 ± 0.15	0.67 ± 0.23 (1×)	2.3 ± 0.2 (3×)	5.3 ± 1.8 (8×)	>250
6q	3.3 ± 1.7	3.5 ± 1.6 (1×)	11 ± 2 (3×)	42 ± 2 (13×)	>250
6r	13 ± 4.2	12 ± 2 (0.9×)	15 ± 4 (1×)	16 ± 7 (1×)	>250
6s	5.3 ± 1.2	4.1 ± 1 (0.8×)	10 ± 2 (2×)	5.3 ± 2.1 (1×)	>100
6t	4.1 ± 1	3.8 ± 1.9 (0.9×)	3.9 ± 2.1 (1×)	16 ± 4 (4×)	>250

[a]Cytotoxic concentration resulting in 50% reduction in the level of ATP in human osteosarcoma (HOS) cells; EC_{50} values obtained from cells infected with lentiviral vector harboring WT or indicated IN mutants as previously reported; [b]Data has been reported previously;[27] [c]Data have been reported previously;[26] [d]Data have been reported previously.[31] [e]FC, fold change relative to WT = EC_{50} of mutants/EC_{50} of WT. [f]Not determined.

65

Table 3. Antiviral potencies in cells infected with HIV-1 vectors that carry DTG-resistant IN mutants.[a]

No.	EC_{50} (nM/FC[c])						
	WT	**G118R**	**T66I**	**E92Q**	**R263K**	**H51Y**	**H51Y/R263K**
RAL (1)[b]	4 ± 2	36 ± 5 (9×)	2.8 ± 0.4 (0.7×)	30 ± 10 (8×)	5.7 ± 2.3 (1×)	3.4 ± 0.2 (0.9×)	6 ± 2.3 (2×)
EVG (2)[b]	6.4 ± 0.8	21 ± 10 (3×)	66 ± 1 (10×)	154 ± 34 (24×)	10 ± 6 (2×)	4.5 ± 2.1 (0.7×)	53 ± 18 (8×)
DTG (3)[b]	1.6 ± 0.9	13 ± 5 (8×)	0.9 ± 0.8 (0.6×)	2.3 ± 0.4 (1×)	11 ± 3 (7×)	3.2 ± 0.2 (2×)	16 ± 2 (10×)
6'b[b]	1.3 ± 0.2	5.3 ± 1.6 (4×)	0.93 ± 0.24 (0.7×)	3.8 ± 2.3 (3×)	2.6 ± 0.1 (2×)	3.8 ± 0.6 (3×)	2.6 ± 1.4 (2×)
6b	1.4 ± 0.4	5.9 ± 1.4 (4×)	0.75 ±0.07 (0.5×)	1.2 ± 0.1 (1×)	1.8 ± 0.3 (1×)	0.8 ± 0.2 (0.6×)	3.9 ± 1.9 (3×)
6p	0.67 ± 0.15	4.8 ± 1.5 (7×)	0.53 ± 0.06 (0.8×)	2.0 ± 1.1 (3×)	0.5 ± 0.0 (0.7×)	0.63 ± 0.30 (0.9×)	2.4 ± 0.8 (0.6×)
6r	13 ± 4.2	24 ± 8 (2×)	1.9 ± 0.07 (0.1×)	6.5 ± 0.8 (0.5×)	18 ± 2 (1×)	11 ± 1.4 (0.8×)	31 ± 10 (2×)
6s	5.3 ± 1.2	15 ± 2 (3×)	1.2 ± 0.5 (0.2×)	3.8 ± 1.3 (0.7×)	3.6 ± 0.9 (0.7×)	7.4 ± 0.9 (1×)	15 ± 1.8 (3×)
6t	4.1 ± 1	4.8 ± 0.6	0.62 ± 0.15	2.7 ± 1.2	6.5 ± 0.8	6.9 ± 2.9	2.5 ± 0.1

		(1×)	(0.2×)	(0.7×)	(2×)	(2×)	(0.9×)

[a]EC_{50} values obtained from cells infected with lentiviral vector harboring WT or indicated IN mutants as previously reported; [b]Data for these compounds have been reported previously.[27, 31] [c]FC, fold change relative to WT = EC_{50} of mutants/EC_{50} of WT.

Table 4. Comparison of antiviral potencies and fold improvement of compounds **6'b** and

6p relative to DTG.

Integrase Mutants	EC$_{50}$ (nM)^a (Fold Improvement^b)		
	DTG (3)^c	**6'b^c**	**6p**
WT	1.6 ± 0.9	1.3 ± 0.2 (0.81 ×)	0.67 ± 0.15 (0.42 ×)
Y143R	4.3 ± 1.2	3.0 ± 0.5 (0.71 ×)	0.67 ± 0.23 (0.16 ×)
N155H	3.6 ± 1.3	2.4 ± 0.8 (0.67 ×)	2.3 ± 0.2 (0.64 ×)
G140S/Q148H	5.8 ± 0.5	9.4 ± 3.6 (1.62 ×)	5.3 ± 1.8 (0.91 ×)
G118R	13 ± 5	5.3 ± 1.6 (0.41 ×)	4.8 ± 1.5 (0.37 ×)
T66I	0.9 ± 0.8	0.93 ± 0.24 (1.03 ×)	0.53 ± 0.06 (0.59 ×)
E92Q	2.3 ± 0.4	3.8 ± 2.3 (1.65 ×)	2.0 ± 1.1 (0.87 ×)
R263K	11 ± 3	2.6 ± 0.1 (0.24 ×)	0.5 ± 0.0 (0.05 ×)
H51Y	3.2 ± 0.2	3.8 ± 0.6 (1.19 ×)	0.63 ± 0.30 (0.20 ×)
H51Y/R263K	16 ± 2	2.6 ± 1.4 (0.16 ×)	2.4 ± 0.8 (0.15 ×)

^{a}EC$_{50}$ values obtained from cells infected with lentiviral vector harboring WT or indicated

IN mutants as previously reported; ^{b}Fold improvement relative to DTG = EC$_{50}$ of

compounds /EC$_{50}$ of DTG. ^{c}Data for these compounds have been reported previously.[27, 31]

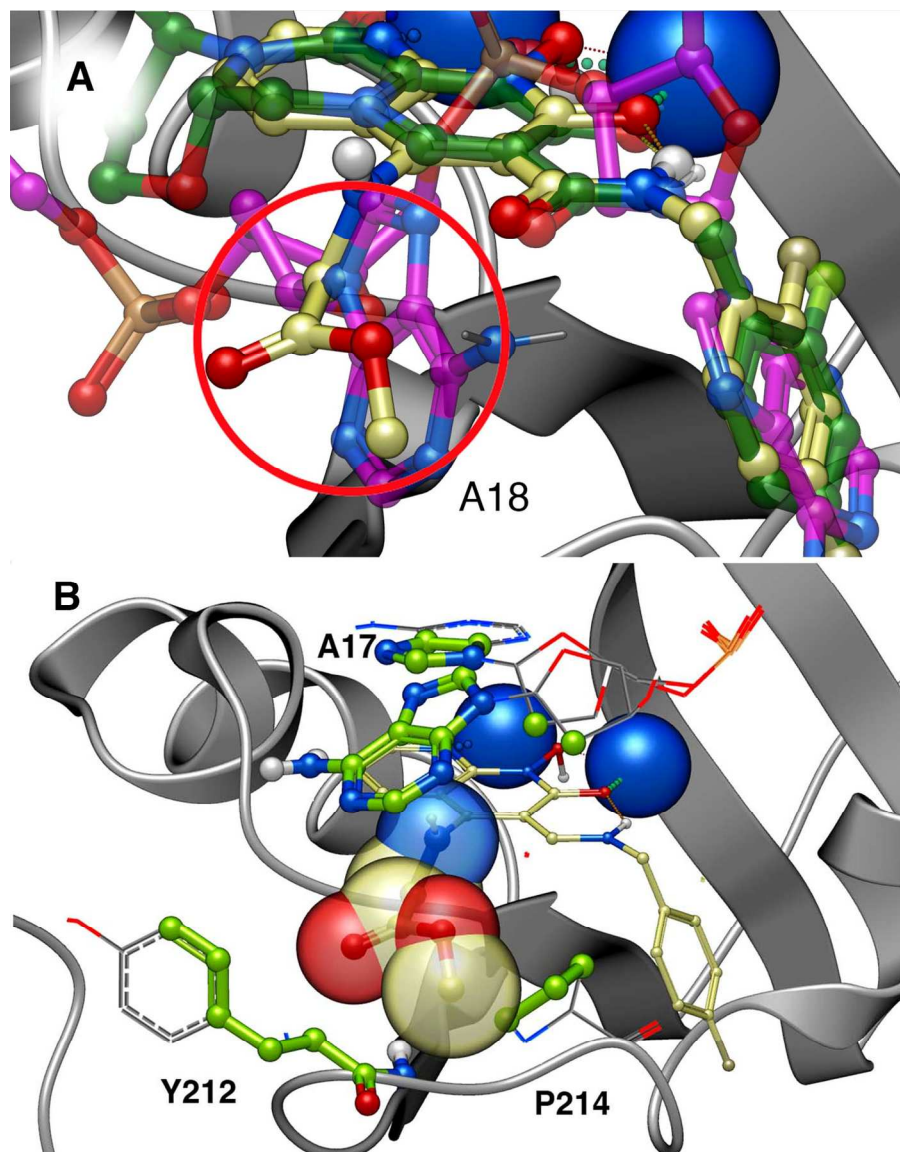**Table 5.** X-ray data collection and refinement statistics.[a]

	5′g	5g	6p
Data Collection			
Space group	$P4_12_12$	$P4_12_12$	$P4_12_12$
Cell dimensions a, b, c (Å)	159.6, 159.6, 124.1	158.6 158.6 123.1	160.5, 160.5, 123.8
Resolution range (Å)	71.36-2.55 (2.62-2.55)	79.29- 2.60(2.67-2.60)	71.77-2.77 (2.84-2.77)
R_{merge}	0.062 (1.49)	0.025 (0.55)	0.072 (1.075)
$I/\sigma(I)$	26.6 (2.0)	19.5 (1.4)	18.9 (2.0)
Completeness (%)	99.8 (98.8)	99.9 (99.7)	98.8 (97.4)
Redundancy	11.5 (11.0)	14.4 (14.2)	7.2 (7.3)
Refinement			
Reflections (total/free)	52,565/2,601	48,670/2,438	40,988/2,057
R/R_{free}	0.179/0.207	0.176/0.204	0.177/0.205
No. Atoms			
Protein, DNA	5,150	5,129	5,127
Ligand	159	132	146
Water	229	109	87
Average B-factors (Å^2)	71.7	84.3	75.7
Protein, DNA	71.3	83.9	74.9
Ligands	91.8	117.23	107.3

69

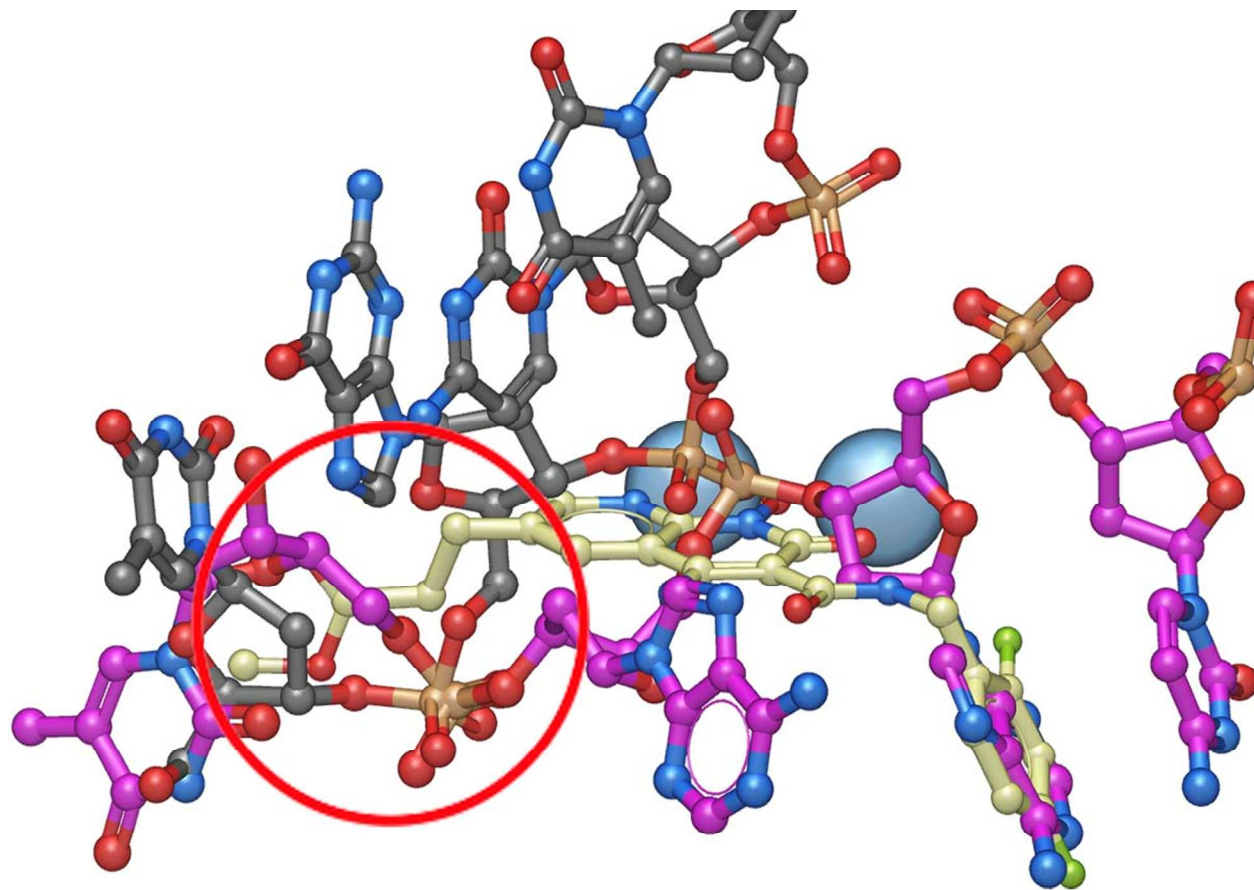|			
Water	67.2	78.9	68.3
R.m.s. deviations			
Bond lengths (Å)	0.038	0.039	0.012
Bond angles (°)	0.56	0.76	1.38
Ramachandran plot (%)			
Favored	99	97	98
Outliers	0	0	0.2

[a]Each structure was determined from a single crystal. Data for the highest resolution shells
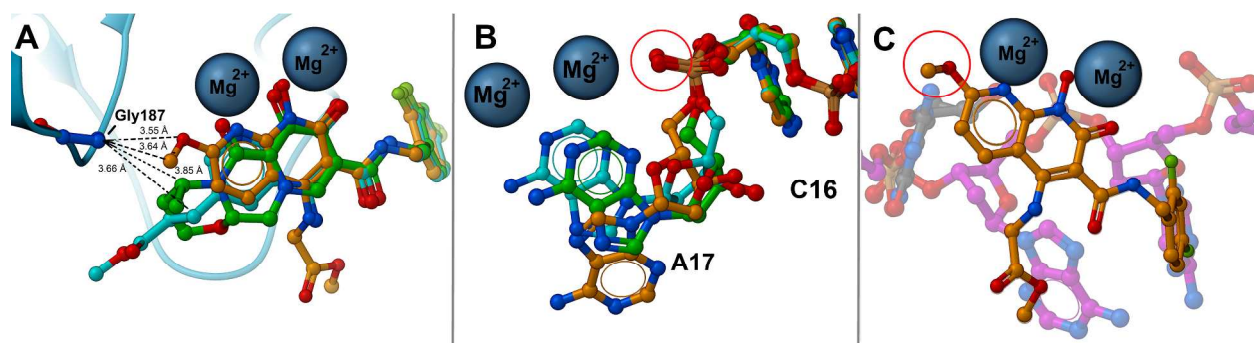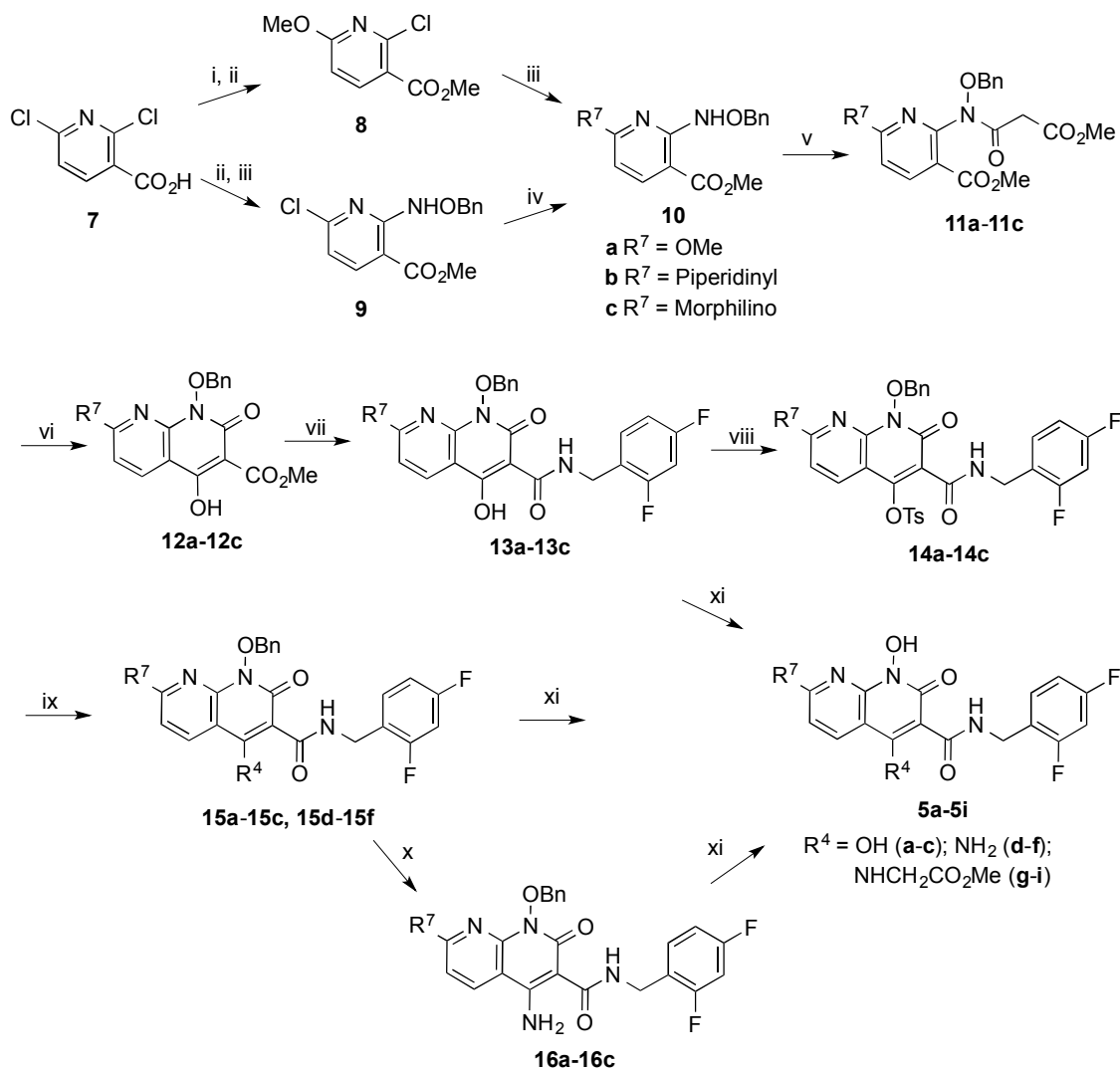
are given in parenthesis.

70

Figure 1. HIV-1 integrase inhibitors. Colored areas indicate regions of intended

correspondence.

71

Figure 2. Crystal structures of PFV intasome – bound inhibitors. (A) Bound **5'g** (cream) with overlays showing the relative positions of pre-3'-P viral DNA (violet; PDB accession code 4E7I) and DTG (**3**) (green; PDB accession code 3S3M). The 4- *N*-(methyl 2-glycinate) moiety of **5'g** is circled in red, highlighting its correspondence with the T_{+2} adenosine (A18) base of pre-3'-P viral DNA; (B) Bound **5'g** with its 4- *N*-(methyl 2-glycinate) moiety shown as transparent spheres. Atoms within 5 Å (Y212 and P214 and A17 of 3'-P DNA) are shown in green as a stick diagram. For both A and B, metal ions are shown as solid blue spheres.

72

Figure 3. Crystal structures of **6p** bound to the PFV intasome. Structures of the pre-3'-P

viral DNA (violet; PDB accession code 4E7I) and target complex host DNA substrate (grey;

PDB accession code 4E7K) are overlaid. The 6-(methyl 3-propanoate) group of **6p** is circled

in red, showing its correspondence with aspects of both pre-3'-P viral DNA and the host

target DNA. Cofactor Mg^{2+} ions are shown as blue spheres; the structures of bound viral

DNAs have been omitted for clarity.

Figure 4. Crystal structures of PFV intasome – bound inhibitors. (A) Bound **5g** (orange) with superimposed **6p** (cyan) and DTG (**3**) (green; PDB accession code 3S3M) showing closest distance to the Gly187 α-methylene (side chains of Asp186 and Gln187 shown in semi-transparent), bound 3'-P DNAs have been omitted for clarity; (B) Superimposed bound 3'-P DNAs associated with Panel A, circled in cyan are the oxygens in the C16– A17 phosphoryl linkages, whose engagement in electrostatic interactions with the side chain imidazole nitrogen of the N224H mutant (corresponding to IN mutant N155H) would be broken on binding of the INSTIs; (C) Bound **5g** with superimposed pre-3'-P viral DNA (violet; PDB accession code 4E7I) and target complex host DNA substrate (grey; PDB accession code 4E7K), circled in red is the 7-OCH_3, which protrudes outside the substrate envelope. Metal ions are shown as solid blue spheres.

Scheme 1. Synthesis of 4,7-Bis-substituted Analogues **5a−5i.** Reagents and conditions: (i)

KO^{t}Bu, MeOH, 65 °C; (ii) H$_2$SO$_4$, MeOH; (iii) BnONH$_2$, DIEA, dioxane, 110 °C; (iv) (b)

piperidine or (c) morpholino, DMF, 80 °C; (v) ClCOCH$_2$CO$_2$CH$_3$, TEA, DCM; (vi) NaOMe,

MeOH; (vii) 2,4-diF-BnNH$_2$, DMF, 140 °C; (viii) TsCl, DIEA, MeCN; (ix) RNH$_2$, DIEA, DMF,

50 °C, R = 2,4-diMeBn (a) or CH$_2$CO$_2$Me (b); (x) TFA, DCM; (xi) H$_2$, 10% Pd/C, MeOH.

Scheme 2. Synthesis of 4,6-Bis-substituted Analogues **6a−6t**. Reagents and conditions: (i)

TsCl, Et$_3$N, CH$_3$CN; (ii) RNH$_2$, DIEA, DMF, 50 °C, R = 2,4-diMeBn (DMP) (a), CH$_2$CH$_2$OH (b),

or CH$_2$CO$_2$Me (c); (iii) Alkyne, Pd(PPh$_3$)$_2$Cl$_2$, DIEA, CuI, DMF, 70 °C or alkene, Pd(OAc)$_2$, TEA,

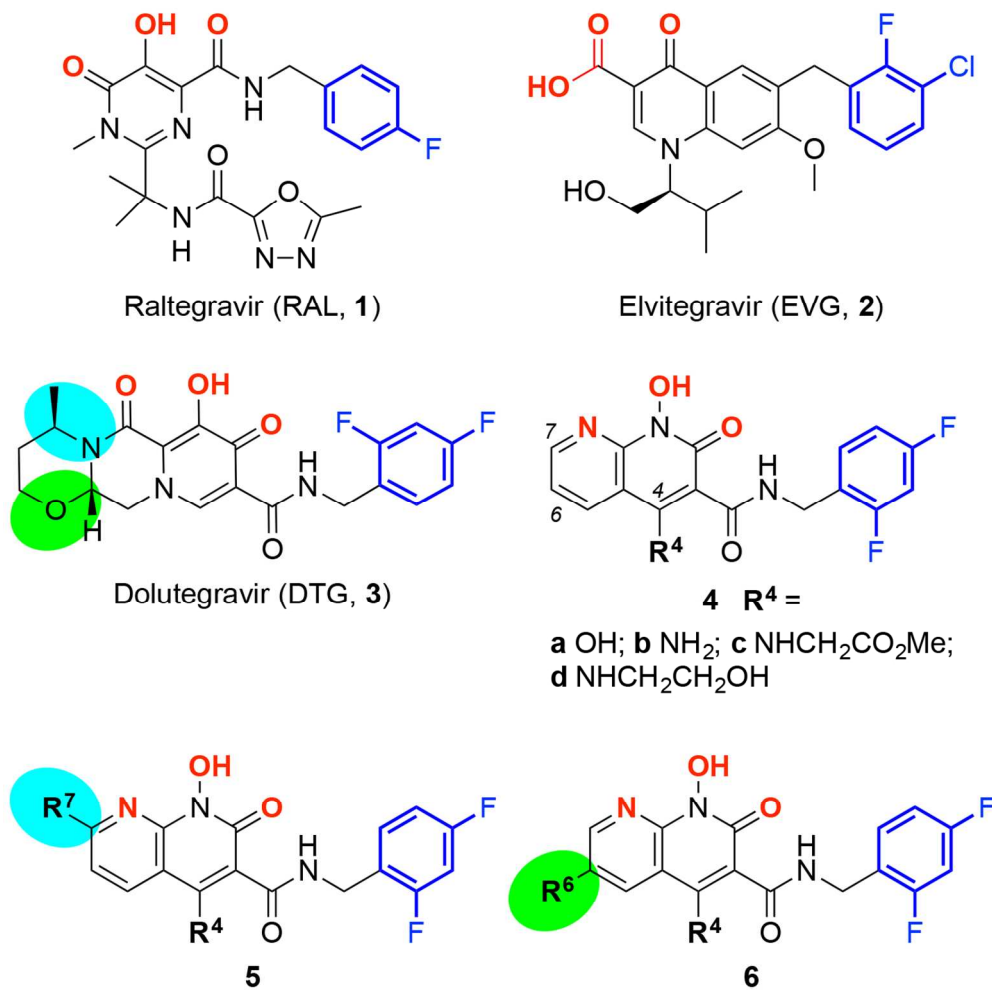PPh$_3$, DMF, 100 °C; (iv) TFA, DCM; (v) H$_2$, 10% Pd/C, MeOH.

Raltegravir (RAL, **1**)

Elvitegravir (EVG, **2**)

Dolutegravir (DTG, **3**)

4 R^4 =

a OH; **b** NH_2; **c** $NHCH_2CO_2Me$;
d $NHCH_2CH_2OH$

5

6
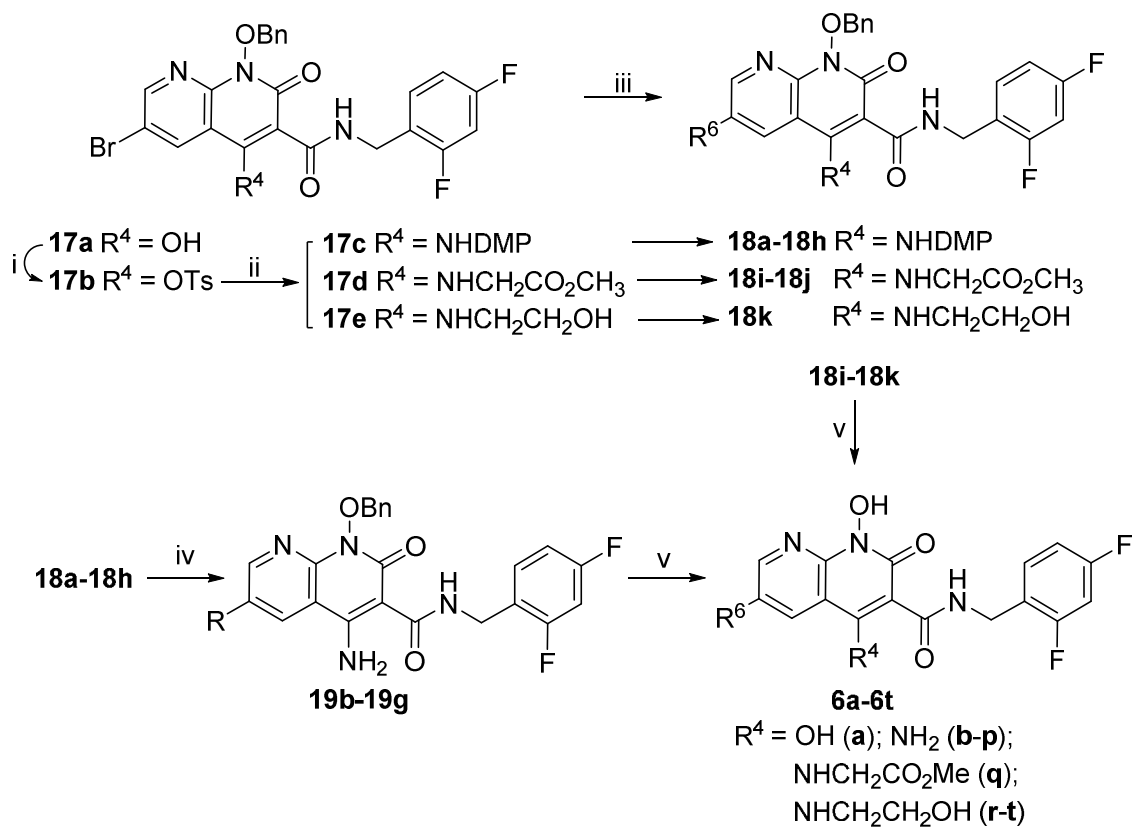
Figure 1. HIV-1 integrase inhibitors. Colored areas indicate regions of intended correspondence.

122x121mm (300 x 300 DPI)
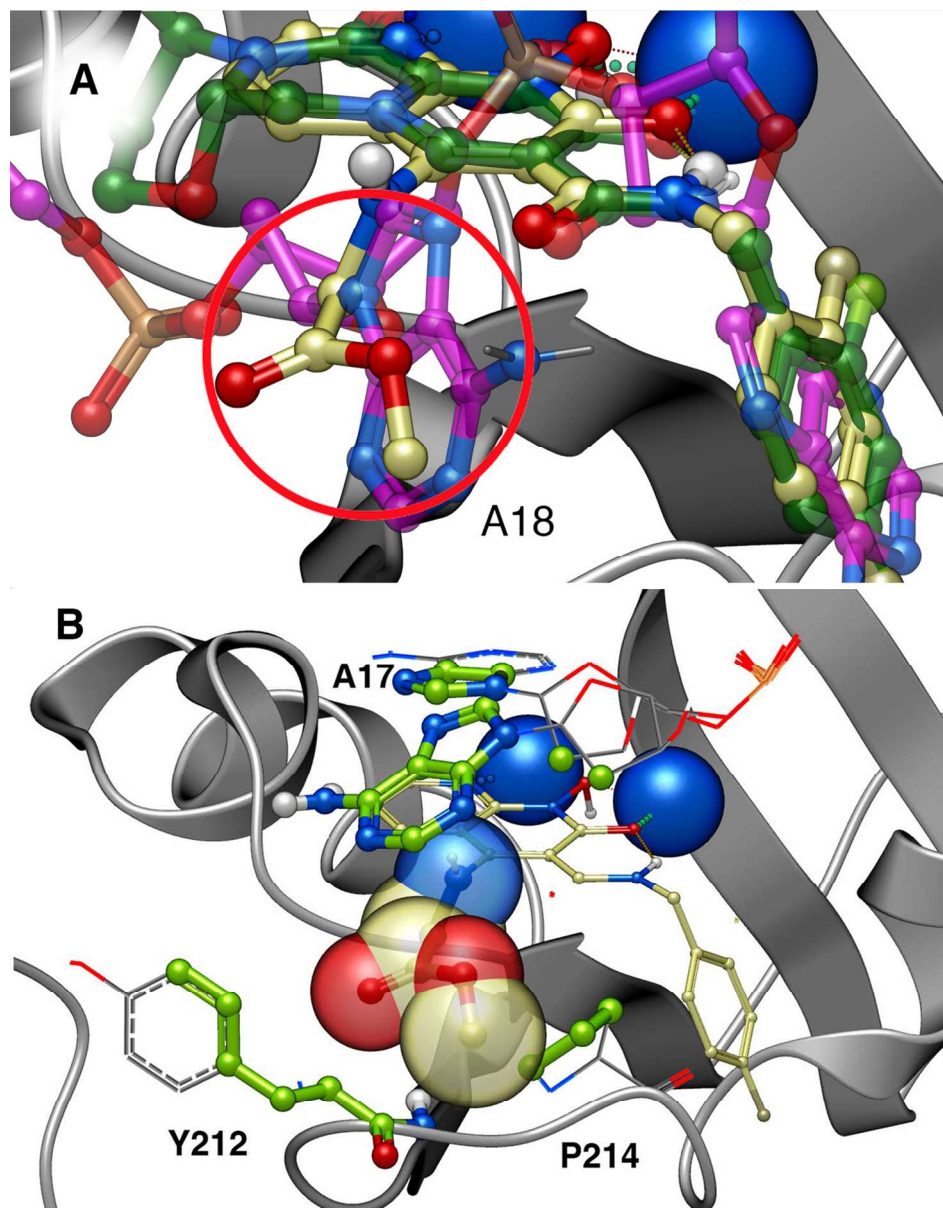
Figure 2. Crystal structures of PFV intasome – bound inhibitors. (A) Bound 5'g (cream) with overlays showing the relative positions of pre-3'-P viral DNA (violet; PDB accession code 4E7I) and DTG (3) (green; PDB accession code 3S3M). The 4- N-(methyl 2-glycinate) moiety of 5'g is circled in red, highlighting its correspondence with the T+2 adenosine (A18) base of pre-3'-P viral DNA; (B) Bound 5'g with its 4- N-(methyl 2-glycinate) moiety shown as transparent spheres. Atoms within 5 Å (Y212 and P214 and A17 of 3'-P DNA) are shown in green as a stick diagram. For both A and B, metal ions are shown as solid blue spheres.

145x185mm (300 x 300 DPI)
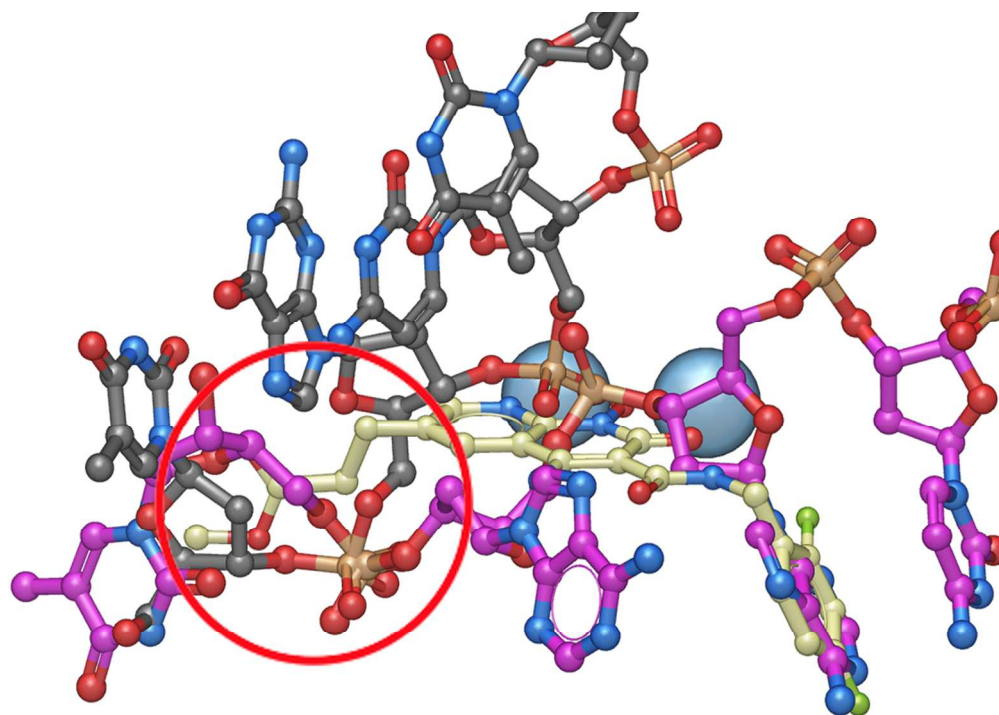
Figure 3. Crystal structures of 6p bound to the PFV intasome. Structures of the pre-3'-P viral DNA (violet; PDB accession code 4E7I) and target complex host DNA substrate (grey; PDB accession code 4E7K) are overlaid. The 6-(methyl 3-propanoate) group of 6p is circled in red, showing its correspondence with aspects of both pre-3'-P viral DNA and the host target DNA. Cofactor Mg2+ ions are shown as blue spheres; the structures of bound viral DNAs have been omitted for clarity.
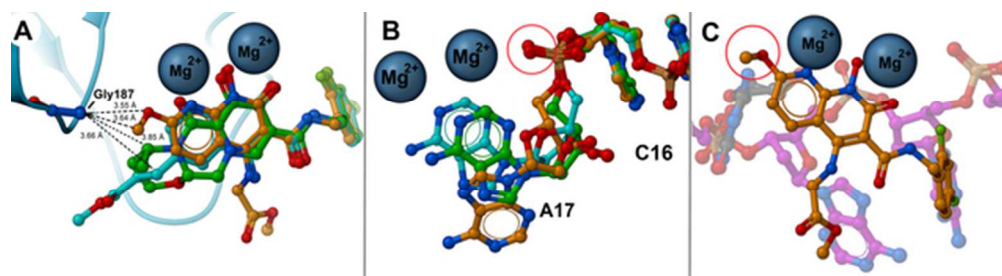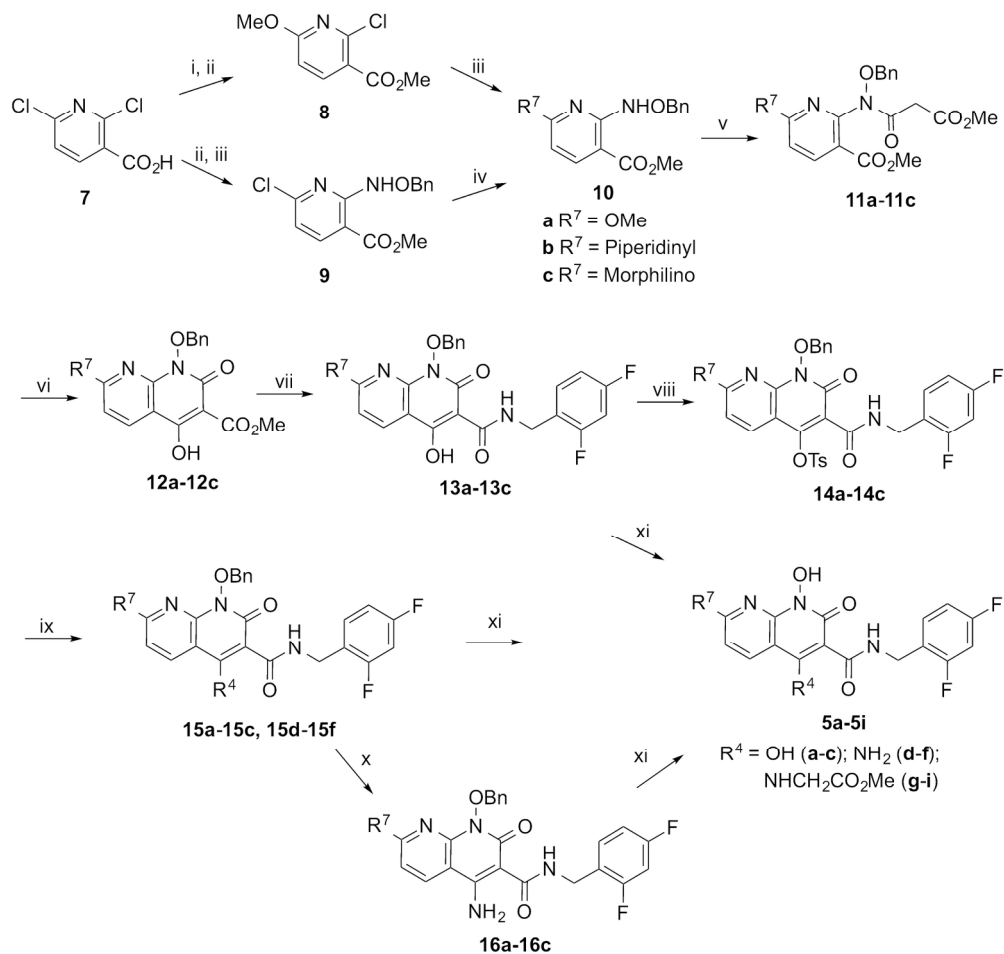
101x73mm (300 x 300 DPI)

Figure 4. Crystal structures of PFV intasome – bound inhibitors. (A) Bound 5g (orange) with superimposed 6p (cyan) and DTG (3) (green; PDB accession code 3S3M) showing closest distance to the Gly187 α-methylene (side chains of Asp186 and Gln187 shown in semi-transparent), bound 3'-P DNAs have been omitted for clarity; (B) Superimposed bound 3'-P DNAs associated with Panel A, circled in cyan are the oxygens in the C16– A17 phosphoryl linkages, whose engagement in electrostatic interactions with the side chain imidazole nitrogen of the N224H mutant (corresponding to IN mutant N155H) would be broken on binding of the INSTIs; (C) Bound 5g with superimposed pre-3'-P viral DNA (violet; PDB accession code 4E7I) and target complex host DNA substrate (grey; PDB accession code 4E7K), circled in red is the 7-OCH3, which protrudes outside the substrate envelope. Metal ions are shown as solid blue spheres.

53x14mm (300 x 300 DPI)

1
2
3
4
5
6
7
8
9
10
11
12
13
14
15
16
17
18
19
20
21
22
23
24
25
26
27
28
29
30
31
32
33
34
35
36
37
38
39
40
41
42
43
44
45
46
47
48
49
50
51
52
53
54
55
56
57
58
59
60

Scheme 1. Synthesis of 4,7-Bis-substituted Analogues 5a−5i. Reagents and conditions: (i) KOtBu, MeOH, 65 °C; (ii) H2SO4, MeOH; (iii) BnONH2, DIEA, dioxane, 110 °C; (iv) (b) piperidine or (c) morpholino, DMF, 80 °C; (v) ClCOCH2CO2CH3, TEA, DCM; (vi) NaOMe, MeOH; (vii) 2,4-diF-BnNH2, DMF, 140 °C; (viii) TsCl, DIEA, MeCN; (ix) RNH2, DIEA, DMF, 50 °C, R = 2,4-diMeBn (a) or CH2CO2Me (b); (x) TFA, DCM; (xi) H2, 10% Pd/C, MeOH.

169x161mm (300 x 300 DPI)
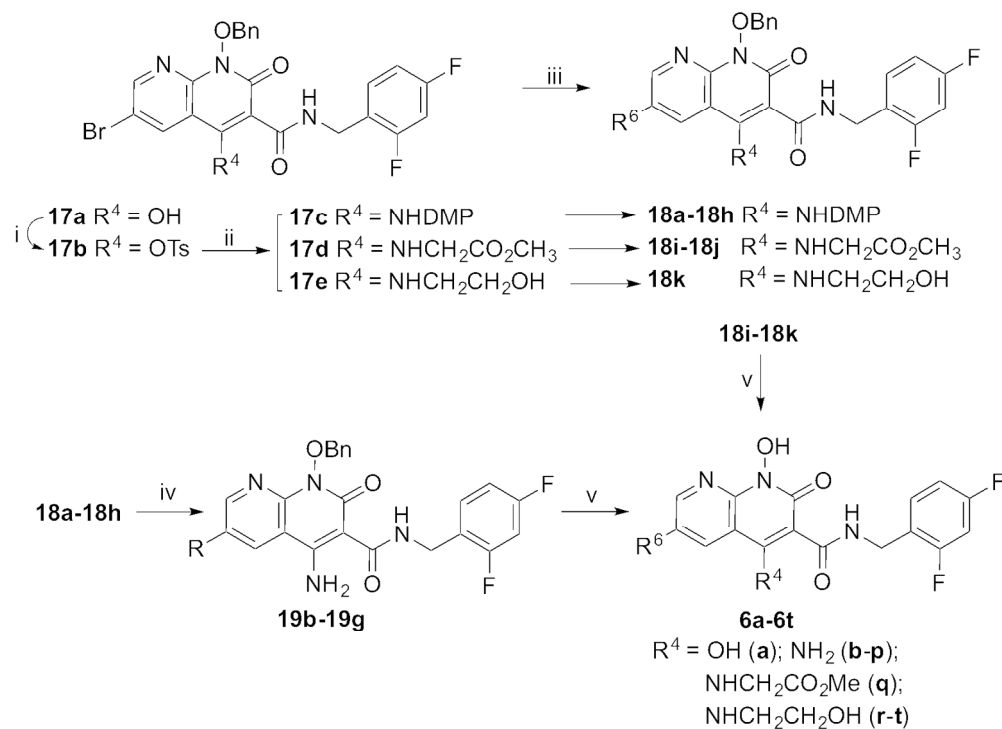
Scheme 2. Synthesis of 4,6-Bis-substituted Analogues 6a−6t. Reagents and conditions: (i) TsCl, Et₃N, CH₃CN; (ii) RNH₂, DIEA, DMF, 50 °C, R = 2,4-diMeBn (DMP) (a), CH₂CH₂OH (b), or CH₂CO₂Me (c); (iii) Alkyne, Pd(PPh₃)₂Cl₂, DIEA, CuI, DMF, 70 °C or alkene, Pd(OAc)₂, TEA, PPh₃, DMF, 100 °C; (iv) TFA, DCM; (v) H₂, 10% Pd/C, MeOH.

150x109mm (300 x 300 DPI)

1
2
3
4
5
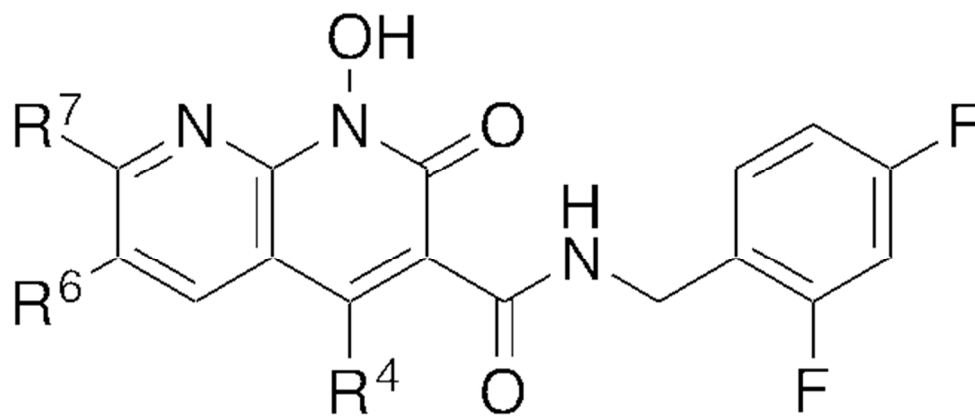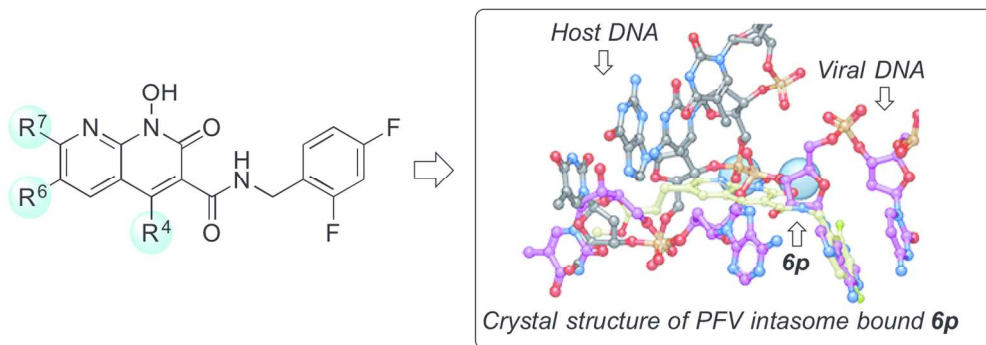6
7
8
9
10
11
12
13
14
15
16
17
18
19
20
21
22
23
24
25
26
27
28
29
30
31
32
33
34
35
36
37
38
39
40
41
42
43
44
45
46
47
48
49
50
51
52
53
54
55
56
57
58
59
60

Table 1 graphic

57x25mm (300 x 300 DPI)

1
2
3
4
5
6
7
8
9
10
11
12
13
14
15
16
17
18
19
20
21
22
23
24
25
26
27
28
29
30
31
32
33
34
35
36
37
38
39
40
41
42
43
44
45
46
47
48
49
50
51
52
53
54
55
56
57
58
59
60

Table of Contents graphic

TOC

144x64mm (300 x 300 DPI)